Norges miljø- og
biovitenskapelige
universitet

**Master's Thesis 2018 30 ECTS**
Faculty of Environmental Sciences and Natural Resource Management

# Hybrid renewable-diesel energy systems in an off-grid arctic community of Svalbard

Oskar Aalde
Renewable Energy – Master's Program

# Preface

This master thesis marks the end of my engagement in the master and bachelor programs within renewable energy offered at NMBU. The courses and events leading up to this conclusion have been academic and co-curricular, both random and planned, challenging and joyful, and I will carry them with me forever. I hope this thesis can supplement, if ever so little, in the process of creating a more sustainable world, and that the skills gained leading up to the thesis submission will be utilized in further endeavors.

I would like to thank Muyiwa Samuel Adaramola for guiding me through the writing process, setting my mind back on track when things seemed complicated, for always having an open door, and for financial support for the simulation software license. Thanks to David Ato Quansah and Vegard Bøe for your HOMER expertise and guidance in the writing process. I pass my appreciation for the wonderful work done by the employees at KINGS BAY AS and researchers at Ny Ålesund for making sure that our arctic regions are being preserved and taken care of for future generations, and a special thanks to the electricians at the power station for showing patience with my many questions and providing data about the energy load in the town. I would also like to offer my gratitude to Andreas Bjørndalen and the Norwegian Scout Association for giving me three wonderful visits to Ny Ålesund and sparking my enthusiasm and love for the region.

Thank you to “Den X-clusive Stiftelse PB”, “Samfunnet i Ås”, and the wonderful class of 2018 for laughter, discussions and companionship. To my parents, I am forever grateful for the support, understanding and comfort you have given me during my stay here at the same university you exited 25 years ago.

Tack psamt PSKAAAL!!!

Ås, May 14, 2018
Oskar Aalde

# Abstract

This thesis examines the viability of using local wind and solar resources in a hybrid renewable-diesel energy system in the off-grid arctic community of Ny Ålesund in Svalbard. The community is the northernmost town in the world with extreme seasonal variations and high degree of remoteness. The analysis has been conducted with load data provided by the local power station manager at Ny Ålesund, and resource data have been collected from BSRN or Satellite databases. The elements added to the existing energy system in the model are (1) wind turbine, (2) solar PV, (3) lithium battery, and (4) inverter. The capital cost for the existing 423 kW diesel generators and boilers were not considered, and a fuel price for diesel was assumed at 9 NOK/litre. The simulation program HOMER was used to conduct the simulations, optimization, and sensitivity analysis. In addition to examining to what degree renewable power sources were economically viable in the current system, cost of achieving 20% renewable energy fraction in accordance with EU targets were investigated.

With no minimum renewable fraction constraints, diesel price at 9 NOK/litre, annual average wind speed at 4,03 m/s and annual average global horizontal irradiation at 1,84 kWh/m2/day, the simulation software found an optimal solution for the energy system in Ny Ålesund with a renewable fraction of 8,9%. Installed wind power capacity was three 100kW turbines and installed sun power capacity was at 470 kW. The annual output from wind power exceeded output from solar power, and the technologies complement each other in terms of seasonal resource availability. The total savings from investing in the energy system presented in this thesis is 15,5 million NOK over the project lifetime of 20 years, and it would reduce diesel consumption by almost 150 m3 annually.

Different sensitivity variables were investigated as part of the system simulation. Net present cost for the project was more sensitive to changes in diesel price, while the renewable fraction was more dependent on wind speed to achieve increase, and solar irradiation in order for it to decrease.

Some challenges occurred in terms of understanding the system element “Thermal Load Controller” used in the simulation software to transform electrical energy to heat energy in the same way as an electric boiler. When activated, the system element changed the outcome of the optimization considerably without any clear correlation to the element’s inputs in price and capacity constraints. Running simulations without considering the capacity and price of the thermal load controller and still allowing transformation of electrical energy to heat energy resulted in substantial reduction in project costs and favored more use of renewable energy with a renewable fraction close to 50% in the most optimal solution.

# Sammendrag

Denne masteroppgaven utforsker mulighetsrommet for bruk av lokale vind- og solressurser til kraftproduksjon i et hybrid fornybar-diesel energisystem i det isolerte arktiske samfunnet Ny Ålesund på Svalbard. Det lille tettstedet er verdens nordligste helårsbosetting og opplever ekstreme sesongvariasjoner og høy grad av isolasjon. Analysen baseres på lastdata fra den lokale kraftstasjonen, og ressursdata er hentet fra BSRN- eller satellittdatabaser. De nye systemelementene lagt til i det eksisterende kraftsystemet er (1) vindturbin, (2) solcellepanel, (3) lithiumbatteri, og (4) inverter. Installeringskostnaden for de eksisterende 423 dieselgeneratorene, oljekjel og el-kjel ble ikke vurdert, og drivstoffprisen er satt til 9 NOK/liter. Simuleringsprogrammet HOMER ble brukt til simulering, optimalisering, og sensitivitetsanalyser. I tillegg til å vurdere til hvilken grad fornybare kraftkilder er økonomisk gunstige tillegg i det eksisterende systemet, ble også kostnaden av å oppnå 20% fornybarandel av all levert energi i henhold til EU-mål for 2020 undersøkt.

Ved ingen gitte krav til fornybarandel, dieselpris på 9 NOK/liter, årlig gjennomsnittlig vindstyrke på 4,03 m/s og årlig gjennomsnittlig global horisontal solinnstråling på 1,84 kWh/m2/dag, ble den optimale systemløsningen for Ny Ålesund gitt med en fornybarandel på 8,9%. Installert vindkraftkapasitet var tre 100kW turbiner, og installert solkraftkapasitet var 470 kW. Den årlige energiproduksjonen fra vindkraft oversteg energiproduksjonen fra solkraft, og teknologiene komplimenterte hverandre godt hva gjelder sesongbasert ressurstilgjengelighet. Den totale innsparingen ved å investere i det presenterte energisystemet er på 15,5 millioner NOK i løpet av prosjektets levetid på 20 år, og dieselforbruket vil reduseres med tilnærmet 150 m3 årlig.

Ulike sensitivitetsvariabler ble undersøkt som en del av systemsimuleringen. Nåverdi for prosjektet var mest sensitiv til endringer dieselpris, mens fornybarandel var mer avhengig av vindstyrken for å oppnå høyere andel, og redusert solinnstråling førte til størst relativ reduksjon.

Noen utfordringer forekom når det gjaldt systemelementet “Thermal Load controller” som brukes av simuleringsprogrammet for å overføre elektrisk energi til termisk energi på samme måte som en el-kjel. Ved aktivering av dette systemelementet ble optimaliseringsresultatet betydelig endret uten noen klar korrelasjon til elementets pris og kapasitet. Ved å kjøre simuleringer uten hensyn til elementets pris og kapasitet, men allikevel tillate transformasjon fra elektrisk til termisk energi viste den optimale løsningen en sterk reduksjon i prosjektkostnad og en fornybarandel tett opp mot 50%.

# Table of Contents

# List of Abbreviations

| | |
|---|---|
| **CO2** | **Carbon Dioxide** |
| **CRF** | **Capital Recovery Factor** |
| **kWh** | **Kilowatt hour** |
| **PV** | **Photovoltaic** |
| **EU** | **European Union** |
| **HOMER** | **Hybrid Optimization Model for Electric Renewables** |
| **LCOE** | **Levelized Cost of Energy** |
| **NPC** | **Net Present Cost** |
| **TLC** | **Thermal Load Controller** |
| **BSRN** | **Baseline Surface Radiation Network** |
| **NASA** | **National Aeronautics and Space Administration** |
| **SRB** | **Surface Radiation Budget** |
| **POWER** | **Prediction of Wordwide Energy Resources** |
| **NOK** | **Norwegian Kroner** |

# 1 Introduction

## 1.1 Background

As the world heads to reach the agreed 2°C degree target in order to mitigate climate gases and transit into a greener energy future, great efforts are needed to replace fossil energy with renewable energy. The power grid serves as the main distributor of energy in urban environments, and in most European countries the grid has been developed in order to reach areas far distance from the power sources. Nevertheless, there are still remote areas or places with an underdeveloped infrastructure that are not able to be supplied with grid-power. These places are forced to find alternative solutions such as off-grid energy systems, and the preferred energy sources have mainly been fossil fuels.

Use of fossil fuels such as gas, refined oil, and coal have several advantages that include: low-effort storage, high energy density, and being easy to transport. Furthermore, these fuels can be divided and fractured in different quantity in order to satisfy a wide range of utilities and their technologies are matured. Notwithstanding of these advantages, fossil fuels comes with a range of hazards for the environment and other disadvantages. These include degradation of local air pollution, global warming through the greenhouse effect of CO2-emission, supply being limited and location sensitive, and the danger of leakage or spill.

With technology advancement, renewable energy sources such as wind and solar, are becoming less costly to utilize and can potentially be a more economical option when designing off-grid energy systems. Furthermore, these technologies come with several other benefits, such as diminishing reliance on external energy providers, no sensitivity to price changes in the market, friendly for climate and local environment, low maintenance and operation costs, and strengthening of the green profile. Nevertheless, renewable energy resources have disadvantages; high investment costs, visual effect in the landscape, and certain technologies might be hazardous for local species such as wind for birds.

When examining advantages and disadvantages of these different energy resources with the rising threat of global warming in mind, it is clear that the renewable energy option is preferable in compliance with the agreed international goals.

In this study, the town of Ny Ålesund on the arctic island Svalbard around 500 km northeast of the Norwegian northern coast is used as example when investigating the possibility of integrating renewable energy into micro-grid communities currently based on fossil fuel energy systems.

## 1.2 Current research on hybrid energy solutions in arctic off-grid systems

According to Green et al. (2017), solar cell technology has experienced steady increase in efficiency during the last two decades. The price per watt installed is at the same time decreasing, and solar power will soon be the cheapest form of electricity in many regions of the world (Mayer et al., 2015). Wind turbine technology is also improving as the global installation is growing rapidly. An increasing variety of small, medium and large sized turbines are entering the market with technology adapted for different conditions and rated power (Islam et al., 2013).

As renewable power production technology is advancing, it has been implemented in a wide range of environments and production costs are decreasing. Installed solar PV capacity is growing rapidly, and with China (78,1 GW), Japan (42,8 GW), and Germany (41,2 GW) topping the list of installed power, around 1,8% of the world's electricity generation was covered by PV power production in 2016 (IEA, 2016). A large proportion of the world population resides in remote regions without profound electricity networks. Many of these communities can gain much from using solar or hybrid energy systems as shown in a comprehensive literature review done by Mandelli et al. (2016). The main focus on the study is power systems in developing areas, but the technologies have also been tested in areas with higher infrastructural development such as the use of solar heating in a project in Drake Landing, Ontario (Sibbitt et al., 2015).The Drake Landing project is after 10 years of operation deemed highly successful, but substantial subsidies were needed to maintain its economic viability.

In Norway, low electricity prices offered on the Nordic grid in addition to high investment costs for renewable energy technology makes it hard for smaller projects to gain present net benefits. Nevertheless, there has been a rising trend in solar instalment in Norway within the last couple of years (Multiconsult, 2016). One reason might be emerging business models such as the one offered by the Norwegian firm Otovo where the firm offers the customer of solar panels a high price for excess electricity produced (Otovo, 2018). Green thinking and the feeling of self-sufficiency might be other factors that are motivating individuals and organizations to investment in solar grid connected systems.

The use and study of solar energy systems at high latitude regions is limited. These regions experience high variations in summer and winter daylight hours, and solar power is therefore not a viable option to keep the energy system for a full year by itself. Still, the amount of irradiation in summer should be as advantageous for production as the low irradiation is a disadvantage in winter. An interesting study done by Obydenkova and Pearce (2016) has shown that nomadic reindeer farmers in Siberia and northern Scandinavia can benefit from adapting solar energy production. In the Siberian case, the farmers could benefit from replacing their diesel aggregates completely, while in the Norwegian case, which was performed at a higher latitude (68°51'N ), showed that solar production could replace fossil power by a great amount.

Implementation and use of wind as energy source in Svalbard is summarized in a report by Kaczmarska et al. (2012). One 20 kW turbine was set up in Hornsund in 1989, but was out of operation within two years due to a blizzard, and another turbine of 1,2 kW was implemented as part of a small off-grid hybrid solar-wind energy system close to Ny Ålesund. The latter rarely reaches rated capacity due to wind speed either exceeding or fall short of needed values. Efforts of wind energy implementation in the arctic regions of Russia are presented in Berdin et al. (2017).

Svalbard has a population of 2 650 people spread in various settlements with most people residing in the city of Longyearbyen. The main island industry has long been coal mining, but after several shut downs, tourism- and research industry are rising as most important activities. Energy demand is expected to rise in accordance with the experienced shift in industry (Eeg-Henriksen & Sjømæling, 2016). Today, Svalbard is mainly provided with energy from diesel generators and coal power plants, and the biggest plant is located in Longyearbyen serving the town with approximately 100 GWh annualy and production divided fairly equally between heat and electrical energy (Traa, 2017). The total emissions from power production on the island are uncertain, but an estimation of 300 000 tonne CO2 was conducted for the year of 2013 (Eeg-Henriksen & Sjømæling, 2016).

Svalbard is on different situation in comparison with mainland Norway when it comes to the issue of energy supply. The island is not connected to the mainland grid and the communities have been dependent on town grids using coal or diesel fuels as their energy source. As the coal mines are shutting down their production, and political willingness to create a greener Svalbard is increasing, alternative power sources are being explored.

For example, solar photovoltaic systems have been installed at rooftops in the towns Longyearbyen and Svea, with the biggest project being the installation of 56 solar panels at the Longyearbyen Airport with installed capacity of 18,3 kW (Sysselmannen, 2016). This is one of many efforts taken by the island's authorities in how the town can reach its goal of replacing 25% of their coal power with renewable energy. In order to contribute in finding greener solutions for Svalbard, this thesis will investigate the viability of introducing a hybrid renewable-diesel energy system in the town of Ny Ålesund.

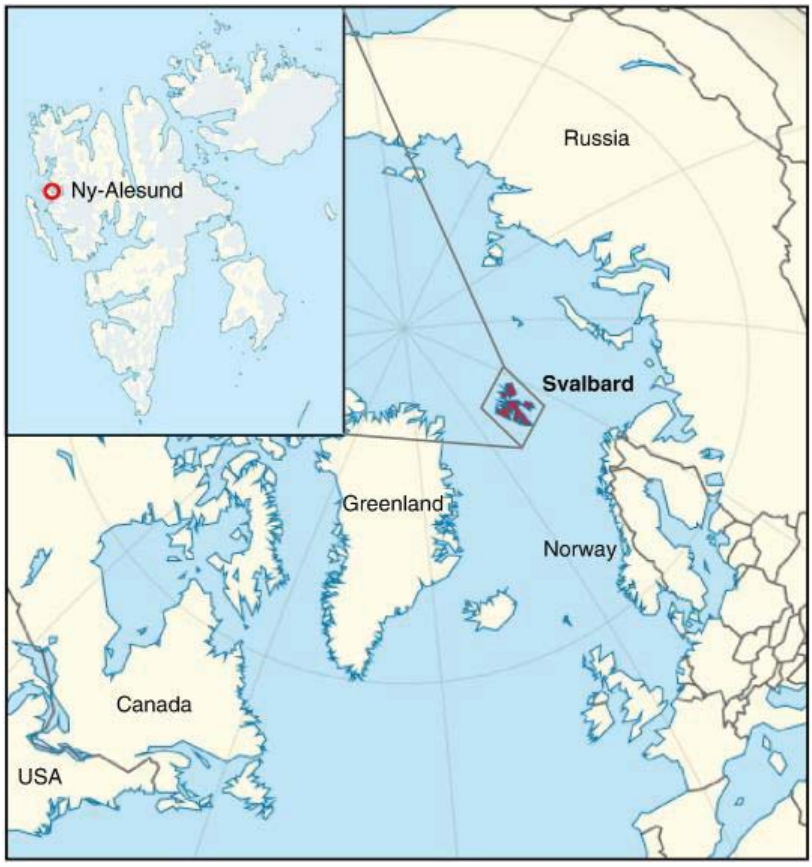


*Figure 1.1: Map indicating the island Svalbard and the town Ny Ålesund. Map gathered from Byun et al. (2014)*

## 1.3 Description of the energy system in Ny Ålesund

A model of the current heat and power electricity system and the proposed changes is presented in figure 1.2. The elements marked with green are the additions made to the system considered in this study, while the white boxes represent the current energy system. Blue arrows signify electrical flows, red arrows signify heat flows, green arrows signify renewable energy, and black arrows signify fossil energy.

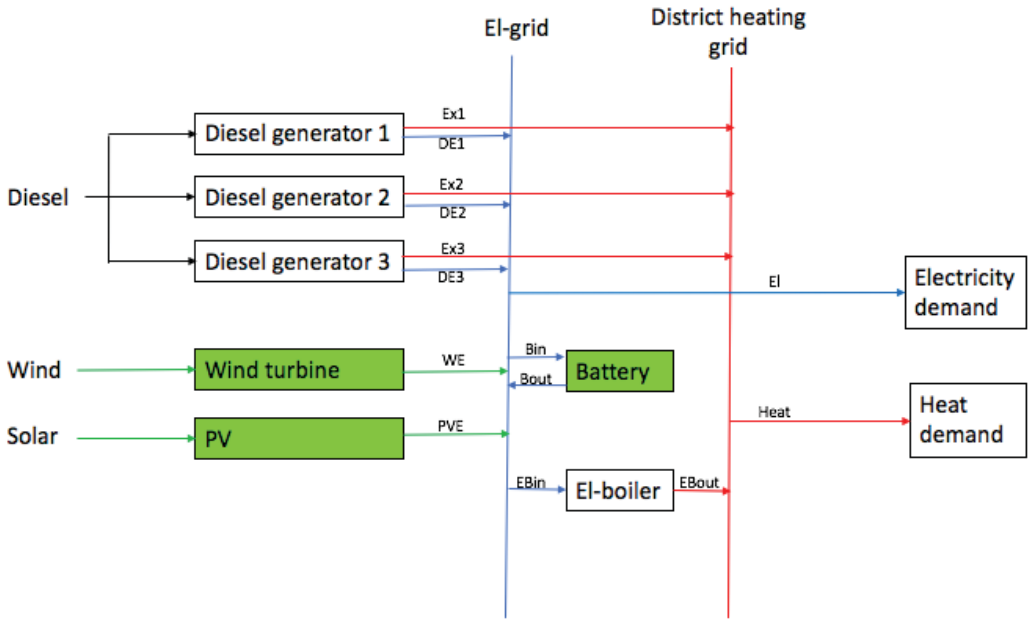


*Figure 1.2: A model displaying the basic elements of the existing energy system in Ny Ålesund as well as the suggested additions. The model is missing the existing diesel boiler that draws from the diesel source and provides the district heating grid with heat energy.*

The heat and electricity demand in the town is served from a centralized power station through the district heating grid and the electric grid. There are also several mobile and decentralized smaller diesel aggregates around the town, but this thesis will only look at the main power generation from the central power station and the connected district heating and electric grid. The sources of power are (1) three diesel generators, each with a capacity of 423 kW, (2) one diesel boiler, and (3) an electric boiler. The diesel generators serve as the main power supply and have a 26,79% heat retrieval rate. A diesel boiler serves the remaining heat load needed in addition to the exhaust recycled heat, and an electric boiler can transfer excess electricity to heat energy when needed. The storage capacity for diesel fuel is at around 1000 m3, and diesel delivery happens twice a year, once in summer season and once in winter season.

By adding new power sources to the system, the diesel consumption can be reduced and hence, reduces emissions from the current energy system. The suggested power sources that will be implemented in this thesis are wind power and solar power. Primarily, both of these power sources will serve the electrical load, and diesel generators will still be needed in order to serve the heat load. It should be noted that wind speed and solar irradiation vary during the day and between seasons, and at times there might be enough excess electricity in the system so that energy from the renewable power sources also can serve the thermal load through the electric boiler.

When both the electrical load and the electric boiler capacity constraint are met by the renewable energy conversion systems (solar and wind), a storage element is needed in order to maximize the use of energy generated by these renewable energy systems. Several storage devices such as hydrogen fuel, heating wells, and batteries could be considered as energy storage facilities. However due to the arctic terrain with permafrost, heating wells would need more research in order for it to be considered, and as batteries are both simpler to integrate in the existing system and more mature as a technology than hydrogen systems, lithium ion batteries were chosen as storage elements in the suggested system.

## 1.4 Thesis Research Question

Answers to the following research questions are to be pursued in this master thesis:

I. *Is it economically viable to implement locally produced solar and/or wind energy in the existing energy system of Ny Ålesund?*

II. *What would be the cost of fulfilling a 20% renewable energy fraction in the town energy system in accordance to the EU goal of 20% renewable in final energy use? What is the cost and viability of fulfilling 50%, 80% and 100% renewable fraction?*

By answering these questions, this thesis will not only provide the town manager “Kings Bay AS” with a possible new solution for their energy system, but also illustrate how arctic communities with limited grid-supply can make use of local energy sources to supply their loads instead of the traditionally used fossil alternatives. By adding the 20% minimum renewable fraction constraint, the thesis will also research the costs of applying the EU 20/20/20 target in a remote community without connection to regional grids. The viability and cost of implementing a system with 50%, 80% and 100% renewable fraction is also explored. As replacing fossil fuels with greener alternatives might have indirect benefits hard to measure in monetary value, it will provide a system cost that can be used as a comparative measure.

# 2 Method

## 2.1 About Ny Ålesund and Svalbard

Ny Ålesund (latitude 78°55'40"N, longitude 11°52'29"E, and elevation 18 meters above sea level) is a town on a remote arctic island with high seasonal variations in climate and daylight (see figure 1.2). After a tragic mining accident in 1962, all mining activity in the town was shut down, and an international research centre for arctic and environmental monitoring was developed to replace activity in the town. Today, over 20 countries are using the town as base for their research, and the facilities and infrastructure are managed by Kings Bay AS. Many of these research projects use sensitive scientific sensors in order to monitor reference values for environmental conditions, and low levels of pollution are beneficial in order to produce accurate results. Kings Bay AS is therefore eager to explore solutions that can minimize the local pollution from sources such as energy production.

In most settlements on Svalbard, as well as in other small remote arctic communities across the hemisphere, diesel or coal generators are the most common source of energy. As renewable options are getting cheaper and the desire to reach international climate targets more acute, much effort is put into researching alternatives to fossil power in the arctic region. Finding solutions for these areas do not only solve local challenges, but also help breaking down the barrier for where to think green. If economically viable renewable energy system solutions can be found for most of these remote and challenging areas, green energy system solutions should be viable all around the globe.

## 2.2 Simulation tool

In order to analyse optimal use of energy sources, the simulation software “HOMER Pro microgrid software” developed by The National Renewable Energy Laboratory (NREL) is used in this study. HOMER is an abbreviation for Hybrid Optimization Model for Multiple Energy Resources, and the software uses inserted resource and financial parameters to solve for most optimal solutions based on inserted system elements (ENERGY, 2018). HOMER has been downloaded by over 80, 000 people in 193 countries since its release in 1993, is constantly updated based on user feedback, and has been used to simulate a wide variety of energy system scenarios (Sinha & Chandel, 2014). It was therefore chosen as the preferred simulation tool for this study.

The software uses a three-step configuration in its model as seen in figure 2.1. In its first step, HOMER simulates to find viable systems that meets the model constraints for all possible combinations of the equipment considered. In the second step, the viable systems are filtered according to some set criteria in order to find the best system optimization. In the third and final step, HOMER will use several optimizations to run a sensitivity analysis investigating the impact of uncontrollable variables (HOMERenergymanual, 2014).

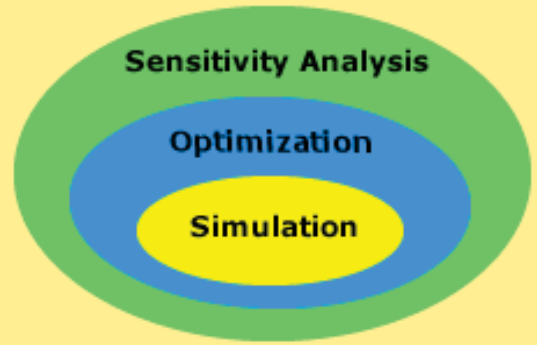


*Figure 2.1: Illustration of the three steps of the HOMER analysis model*

For this thesis, Homer Pro standard version in addition to the "combined heat and power module" were used. The "combined heat and power module" makes it possible to optimize for an energy system with both a heat load and an electrical load, and it makes additional system elements such as a "boiler" and "Thermal load controller" accessible. Furthermore, the added module makes it possible to convert excess electricity into heat energy serving the thermal load, and a "heat recovery ratio" is added to the diesel generators (HOMERenergymanual, 2014).

### 2.2.1 Configurations, optimization and sensitivity variables

Different scenarios were considered when simulating for viable energy system solutions. All system elements were alike in all scenarios, but different constraints for the renewable fraction in the energy mix were set for different simulation runs in order to find the optimal solution solely based on monetary value, and different optimal solutions for various ambitions on renewable targets.

The optimization goal for the energy system in Ny Ålesund is to find the lowest possible net present cost (NPC) within the model limit. HOMER software achieves this by filtering all viable solutions subject to imposed constraints so that the system with the lowest NPC gets the highest ranking. Based on different configurations in the original system, the software would then present the highest-ranking system solution for each configuration.

Time was a limiting factor when deciding which variables to consider in the sensitivity analysis for the energy system. When running more than three variables in the analysis, the estimated time for simulation lasted more than 24 hours. For that reason, average annual solar irradiation, average annual wind speed and diesel price were selected as the three variables to be included with a positive and negative percentage change in input value of 25%, 25%, and 50% respectively. The annual average solar irradiation and annual average wind speed were chosen due to the uncertainties that will be explained in chapter 2.3.2 and 2.3.3.2, and diesel price as there is high uncertainty on further price fluctuation in crude oil price and it being the main variable cost in the simulation (Bøhnsdalen et al., 2016).

## 2.3 Load

### 2.3.1 Monthly electrical and thermal loads

Accurate load data is important in order to design a system able to meet the load demand for heat and electricity at any given time of the year. For the community in Ny Ålesund, two loads are to be considered, which are thermal load and electrical load. In the existing system both loads are served and kept in balance from the local power plant managed by two electricians. After communication by mail, energy production logs from 2012 to 2017 were accessed. The load data for electrical and thermal energy delivered were separated into months, and monthly averages were calculated as shown in figure 2.2. The spreadsheets were at times hard to interpret without full insight in abbreviations and report schedule, and there were also several errors that were hard to figure out without laborious communication with the electricians operating the powerhouse. For that reason, time series with values that seemed strange or lacking in comparison to the other values were excluded from the data collection.

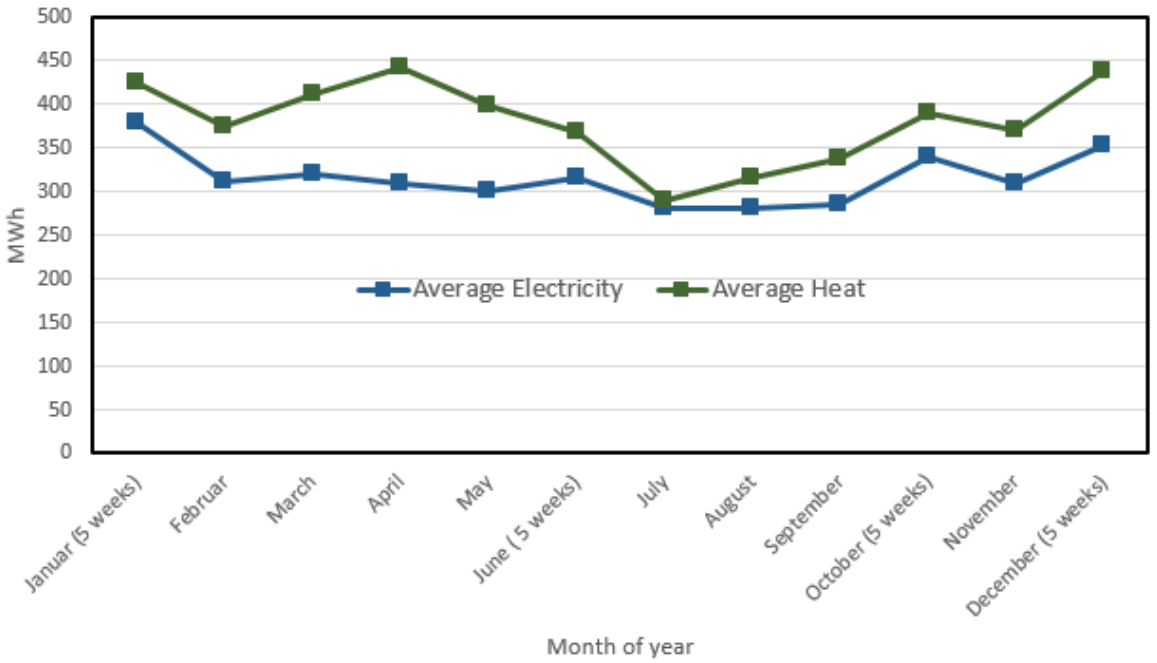


*Figure 2.2: Average monthly thermal and electricity loads in Ny Ålesund from 2012 to 2017 as given by the Ny Ålesund power station manager*

As can be observed from Figure 2.2, the consumption is fairly equally distributed over the year with a slight dip in the summer months May to August. This trend seems more distinct for the heat load than the electricity load, and it is probably caused by correlation to outside temperature. The average daily loads for electricity and heat are 10 355 KWh and 12 485 KWh respectively. Average annual monthly load is 314,96 MWh for electricity and 379,76 MWh for district heating with monthly max load at 379,01 MWh (Jan) for electricity and 441,34 MWh (Apr) for district heat, and minimum load at 280,40 MWh (Aug) for electricity and 290,36 MWh (Jul) for district heat. The load data was inserted in the programming software, and figure 2.3 and 2.4 displays how the software handles load variety. For both figure 2.3 and 2.4, the line at the top and bottom for each month show the monthly maximum and minimum values respectively. The blue line at the top and bottom of the blue box show the average daily maximum and minimum value for each month. The middle line shows the average monthly load.

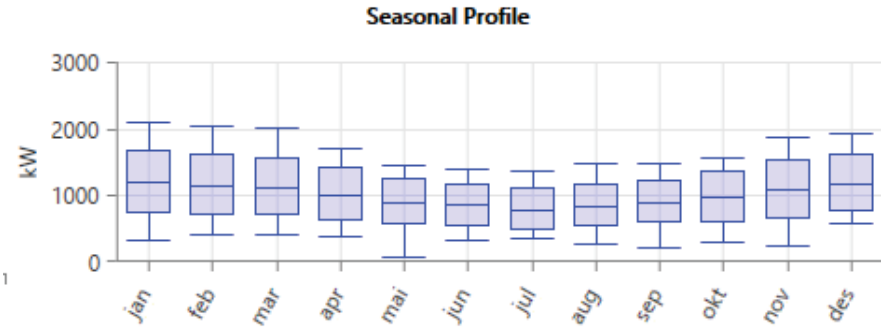


*Figure 2.3: Annual heat load curve as shown in HOMER*

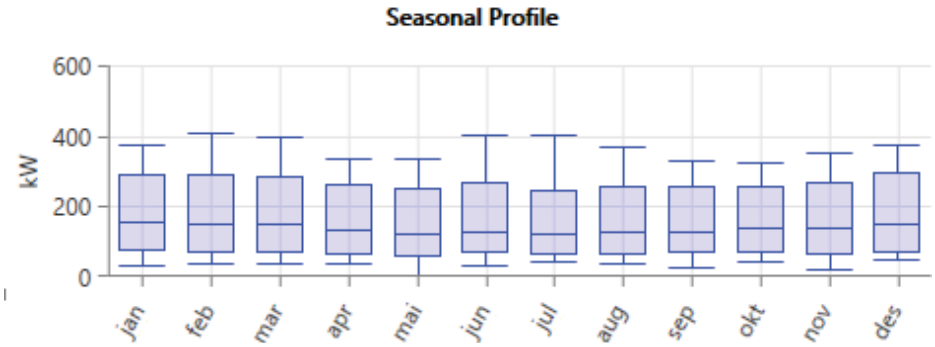


*Figure 2.4: Annual electrical load curve as shown in HOMER*

A daily load curve should be estimated in order to better optimize the system in terms of energy balance. Renewable power production fluctuates according to sun availability and wind strength, and furthermore, the power consumption varies as different energy services are activated during the day. As renewable energy from sun and wind must be used at the same time as it is produced if not stored in batteries or other storage devices, it is essential to size renewable energy conversion systems so that it can best follow the daily demand curve. The load data received from the electricians at Kings Bay did not contain any information on daily load consumption, so a daily load curve must be assumed based on advice from the power station manager and knowledge about how the inhabitants behave during a day. As Ny Ålesund is operated with centralized cafeteria, welfare room, washing facilities and other community services, most of the electrical energy is used during worktime from 07.00 – 16.00.

The simulation tool used in the thesis offers three standard daily power curves in addition to a flat consumption curve; a residential curve, an office curve, and a community curve. The office pattern shown in figure 2.5 was chosen due to the similarity between the community and an office environment.

A flat daily load pattern as shown in figure 2.6 is assumed for the heat load as heating is kept fairly constant during the day and night through the district heat system. Furthermore, it is assumed that all weekdays follow the same consumption pattern and load curve, as there is not much difference in the energy intensive activity between working days and weekends. It is reasonable to believe that the activity goes slightly down during weekends, but due to lack of proper data, an equal daily load curve for all weekdays is chosen.

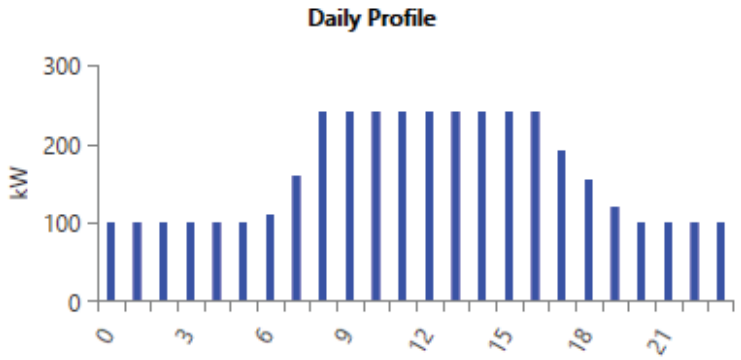


*Figure 2.5: Daily load profile curve for the electrical load as shown in HOMER*

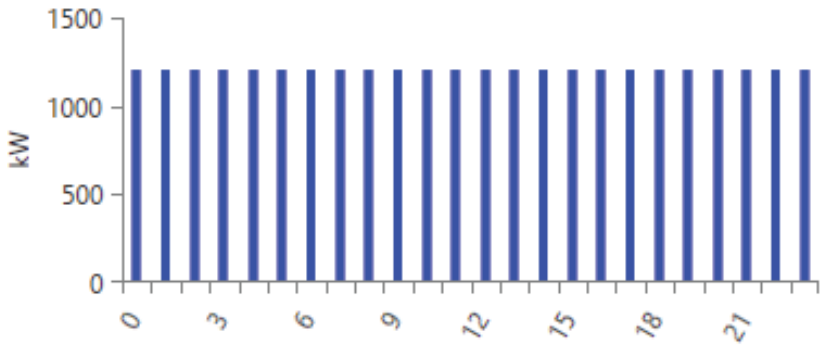


*Figure 2.6: Daily load profile curve for the heat load as shown in HOMER*

### 2.3.2 Seasonal variations

Ny Ålesund experiences great environmental variations in daylight and temperature between winter and summer, and it is natural to assume that the daily consumption curve and seasonal loads should vary between the seasons. The site experiences polar night from 24$^{th}$ of October to 18$^{th}$ of February and polar day from 18$^{th}$ April and 24$^{th}$ of August due to its high latitude of around 79°N (Maturilli et al., 2015), and hence the sun never rises above the horizon or never sets respectively during these periods.

In addition, the average temperature in winter is substantially lower than for the summer months, leading to higher demand for electrical services such as light and greater demand for heating power in the winter season compared to summer. A way of modelling this is to differentiate between three daily load curves for the three different seasonal patterns; winter, summer and mid-season (fall and spring). After considering how scientific activity in the town also varies greatly throughout the year, this does not seem necessary. The town population is reduced from around 180 inhabitants in summer to around 30 in the winter months, and this reduction in people makes up for the increase in energy services needed in winter. In figure 2.2, a slight rise in energy usage for both electricity and heat is shown for the winter season, but the spikes of the daily curve are assumed to remain somewhat the same.

## 2.4 Renewable energy resources

The hybrid energy system is designed to consist of renewable energy conversion technologies and diesel generators as well as energy storage facility. For the renewable energy conversion technologies, three main parameters, which are wind strength, global solar radiation and ambient temperature, are required to calculate energy yield from the considered technologies which are wind turbine and solar photovoltaic panels.

### 2.4.1 Sources for meteorological data

Two data sources have been used to gather the needed weather data used in the simulations. The most accurate source is the baseline surface radiation network (BSRN) station located in Ny Ålesund. Fifty nine (59) BSRN stations are spread across the globe and gathers detailed data on a variety of environmental parameters such as temperature, solar irradiation and wind strength (BSRN, 2018). Access to the BSRN database required access to a unique toolbox called “BSRN toolbox” (PANGEA, 2018), but due to time limitations, the effort needed to understand and manage data through the toolbox exceeded its gains. Instead, BSRN datasets within limited time periods were accessed through various scientific papers. Data from NASAs surface radiation budget (SRB) database was used as solar irradiation input as sufficient BSRN values were inaccessible.

The SRB contains global 3-hourly, daily, monthly/3-hourly, and monthly averages of surface and top-of atmosphere longwave and shortwave radiative parameters on a 1°x1° grid (NASA, 2018). Model inputs of cloud amounts and other atmospheric state parameters are also available in some of the data sets. These 3-hour time step data are monthly averaged from 22 years of satellite monitoring. Data was acquired from the “prediction of worldwide energy resources” (POWER) home page.

The data simulation software HOMER can automatically download these datasets as its resource parameters. The downloaded files in HOMER were validated with the data acquired from POWER (POWER, 2018).

### 2.4.2 Wind data

Wind speed, hub height, and air density are important factors in calculating how much power a turbine can produce under given conditions.

The HOMER software calculates power output in three steps. First, it calculates the wind speed at the hub height of the wind turbine based on measured wind data, then calculates how much power the wind turbine produces at hub-height wind speed at standard air density and finally, adjusts that power output value for the actual air density at the project location.

Figure 2.7 graphically displays the wind strength data used in this simulation. There is a clear trend showing higher values for the annual monthly average wind speed in winter and lower values in summer. This supports a hybrid renewable energy solution as solar radiation has an opposite trend considering seasonal energy source availability.

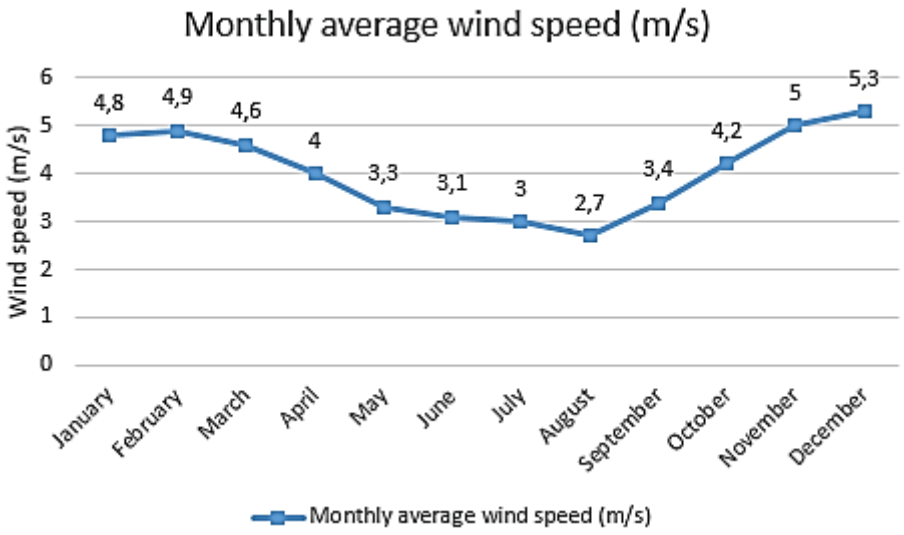


*Figure 2.7: Annual monthly wind speed*

The wind data is based on annual monthly averages for the time period of 2005 to 2016 measured by the French - German arctic research center AwiPew which operates the BSRN station in Ny Ålesund (Cisek et al., 2017). As shown in figure 2.7, values for average monthly wind speed lie between a maximum of 5,3 m/s in December and a minimum of 2,7 m/s in August.

The annual daily average wind speed is at 4,01 m/s. Previous measurements between the years 1975 and 2000 show an annual daily average wind speed of 2,6 m/s (Przybylak & Arazny, 2006). According to the Norwegian meteorological institute, the annual daily average wind speed for the previous 12 months was 3,58 m/s (YR, 2018). In order to adjust for uncertainties in predicting future wind speed, the variable was added as a sensitivity factor considering a 25% negative or positive deviation in annual daily average wind speed.

The wind speed was measured at ten (10) meters above ground. As the areas around Ny Ålesund mainly consists of tundra with little or no vegetation, the ground conditions are set to "rough pasture" with a surface roughness length of 0,01 (Manwell et al., 2010). The hub height of the turbine is the height used for calculating wind power output. The hub height for the XANT-21 100kW turbine used in this simulation is thirty-one (31) meter, and the wind measurements have to be adjusted accordingly. There is mainly two different ways of scaling measured wind to hub height; a logarithmic scale and a power law profile. Logarithmic scale was chosen for this analysis using equation 2.1 for conversion.

$$U = U_{known} * \frac{ln\left(\frac{z}{z_o}\right)}{ln\left(\frac{z_{known}}{z_o}\right)} \tag{2.1}$$

Where:

$U$: Wind speed at hub height [m/s].

$U_{known}$: Wind speed at anemometer height [m/s].

$Z$: Hub height of wind turbine [m]. Set to 31 meters.

$z_{known}$: Height of anemometer [m]. Set to 10 meters.

$z_o$: Surface roughness length [m]. Set to 0,01 meter.

After HOMER determines the hub height wind speed with equation 2.1, it refers to the wind turbine's power curve in order to calculate the expected power output. The power curve shows energy output levels for a specific wind turbine at different wind speed under standard conditions of temperature and pressure. If the wind speed at the turbine hub height is outside the range defined in the power curve, the turbine produces no power, following the assumption that wind turbines produce no power at wind speeds below the cut-in or above the cut-out wind speeds. In figure 2.8, the power curve for the XANT-21 100kW wind turbine used in the analysis is shown (XANT, 2018).

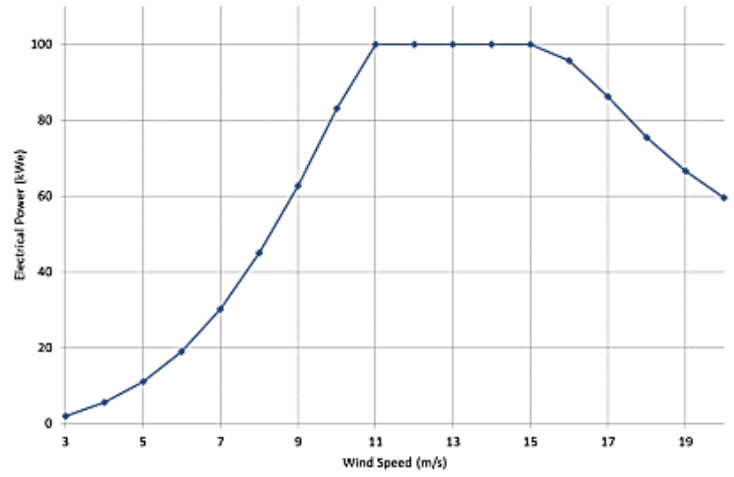


| Wind Speed (m/s) | Power (kWe) |
|---|---|
| 3 | 1.97 |
| 4 | 5.61 |
| 5 | 10.97 |
| 6 | 19.98 |
| 7 | 30.14 |
| 8 | 44.99 |
| 9 | 62.6 |
| 10 | 83.09 |
| 11 | 100.0 |
| 12 | 100.0 |
| 13 | 100.0 |
| 14 | 100.0 |
| 15 | 100.0 |
| 16 | 95.7 |
| 17 | 86.24 |
| 18 | 75.45 |
| 19 | 66.52 |
| 20 | 59.59 |

*Figure 2.8: Power curve for the XANT-21 100 kW under standard test conditions*

As seen in the power curve, the XANT-21 100kW has a cut-in wind speed at 3 m/s and a cut-out wind speed at 20 m/s. The rated wind speed of the turbine is 11 m/s meaning that it produces at maximum capacity (100kW) from this wind speed and onwards until it reaches 15 m/s.

In the last step for calculating power from wind, the software adjusts the power output found from the turbine power curve with the site-specific air density. HOMER uses altitude as its only input for calculating air density, and there is no possibility for manually inserting values. The altitude above sea level for the turbine was set at 35 meters, the same height as the local airport.

$$\frac{p}{po} = \left(1 - \frac{Bz}{To}\right)^{\frac{g}{RB}} \left(\frac{To}{To - Bz}\right) \tag{2.2}$$

Where:

$\frac{p}{po}$: Air density ratio of site-specific air density ($p$) and standard air density ($po$) = 1,225kg/m3

$B$: Lapse rate [0,00650 K/m].

$z$: Altitude above sea level [m]. Set to 35 in this analysis.

$To$: Temperature at standard conditions [288,16 K].

$g$: Gravitational acceleration [9,81 m/s2].

$R$: Gas constant [287 J/kgK].

Using equation 2.2, air density is calculated at p = 1,22088 kg/m3 and the air density ratio at 99,66%. As Svalbard experiences cold temperatures way below the standard test conditions at 20 degrees, the equation used by HOMER is not able to calculate air pressure accurately with only altitude as its input. In order to find the impact of the limitation in equation 2.2, the monthly average temperature and air pressure data from Maturilli et al. (2015) was used to calculate air density more accurately using the ideal gas law as shown in equation 2.3.

$$Pdry\ air = \frac{p}{RT} \tag{2.3}$$

Where:

Pdry air: Density of dry air [kg/m3].

$p$: Air pressure [Pa].

$R$: Gas constant [287 J/kgK].

$T$: Site specific temperature [288,16 K].

The calculated annual average air density for Ny Ålesund using the ideal gas law is at 1,308 kg/m3. The more correct air density ratio is thus at 106,77% which means that the modelling software undervalues the wind performance with its calculated value of 99,66%. This factor adds to why wind speed should be included as a sensitivity variable.

In the last step of calculating wind turbine power output, the air density ratio is used to adjust for the wind turbine power output found in the turbine power curve as shown in equation 2.4.

$$P_{WTG} = \left(\frac{p}{p0}\right) * P_{WTG,STP} \tag{2.4}$$

Where:

$P_{WTG}$: The wind turbine power output [kW].

$P_{WTG,STP}$: The wind turbine power output at standard temperature and pressure

$p$: Air density calculated by HOMER [1,2208 kg/m3]

$p0$: Air density at standard temperature and pressure [1,225 kg/m3]

### 2.4.3 Solar resource and temperature data

The equation for calculating PV array power output for each time step is given in equation 2.5 (HOMERenergymanual, 2014).

$$E_{PV,T} = Y_{PV} f_{PV} \left(\frac{\bar{G}_T}{\bar{G}_{T,STC}}\right) [1 + \alpha_p (T_{c,T} - T_{c,STC})] \quad (2.5)$$

Where:

$EPV,T$: Power output in current time-step [kW]

$YPV$: Rated peak capacity of the array under standard test conditions [kW]

$fPV$: Derate factor of the array [%]

$\bar{G}T$: Irradiance incident on the PV array in current time-step [kW/m2]

$\bar{G}T,STC$: Irradiance incident on the PV array under standard test conditions [1kW/m2]

$\alpha p$: Temperature coefficient of power [%/°C]

$Tc,T$: Cell temperature in current time-step [°C]

$Tc,STC$: Cell temperature under standard test conditions [25 °C]

The amount of solar irradiance in the current time-step ($\bar{G}T$) decides how fast the solar cells in the array is able to excite electrons and create electrical energy. This process is affected by the cell temperature, and the temperature coefficient of power ($\alpha p$) indicates how much the PV array power output depends on change in temperature change.

#### *2.4.3.1 Temperature data*

The PV cell temperature in the current time-step ($T_{C,T}$) is calculated from the ambient temperature at the model location. The temperature resource data used as input in the simulation software is gathered from the BSRN database at Ny Ålesund. The dataset contains the monthly average surface air temperature in the period August 1993 to July  and was made available in a study by Maturilli et al. (2015). Figure 2.9 presents the annual monthly temperatures graphically.

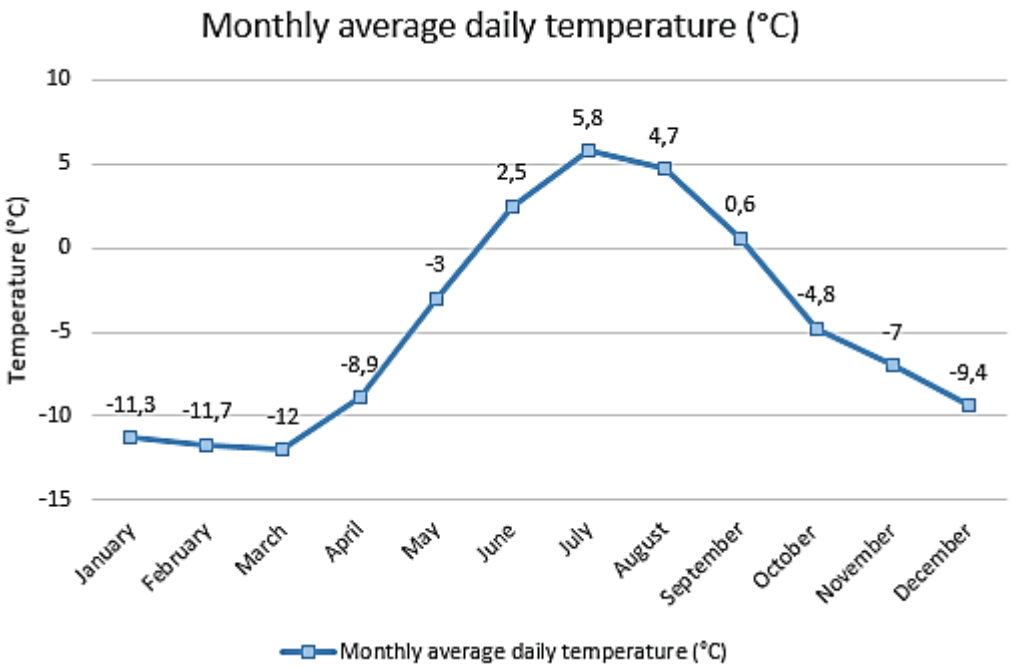


*Figure 2.9: Annual monthly average temperature in Ny Ålesund*

As seen in figure 2.9, the monthly average temperature in Ny Ålesund is at a maximum in July at 5,4 degrees Celsius and at a minimum in March at -12 degrees Celsius. The annual average is at -4,54 degrees Celsius, far below the standard test condition of 20 degrees for PV. Lower ambient temperatures lowers the temperature of the cells in the solar panels, giving them higher power yields according to the temperature coefficient of power as shown in equation 2.5.

The BSRN annual average temperature is almost two degrees Celsius higher compared to the normal values presented by the Norwegian meteorological institute from their weather station in Ny Ålesund measured between 1961 and 1990 (YR, 2018).An article by Førland et al. (2011) show that Ny Ålesund has experienced an increase of 0,99 degrees Celsius per decade in the period 1989 to 2011, which aligns well with the difference in average annual temperature from the two data sources considering their time-scopes. As the average one-year temperature between April 2017 and April 2018 was measured to -2,04 degrees Celsius by the Norwegian meteorological institute, it is reasonable to believe that the annual temperature on Svalbard keeps on increasing. A one-year average was not deemed sufficient as input value due to its short time-scope, and the BSRN measurements were therefore used as temperature resource in the system simulation.

#### *2.4.3.2 Solar radiation data*

Ny Ålesund's high latitudinal position implies polar night condition between October 24$^{th}$ and February 18$^{th}$, and polar day between April 18$^{th}$ and August 24$^{th}$, respectively (Maturilli et al., 2015).

The solar resource is available for twenty-four (24) hours per day during polar day and zero hours during polar night, which gives Ny Ålesund substantial seasonal variations in the solar resource. Solar radiation energy can be transformed to electrical power through solar photovoltaic modules. In order to assess PV energy output, solar radiation resource data must be measured and put into the simulation. The available radiation is measured in irradiance (w/m2) and irradiation (kwh/m2). Irradiation is usually given as unit per day, and thus measured in kWh/m2/day. Total global irradiance ($\bar{G}$) is found through equation 2.6.

$$\bar{G} = \bar{G}d + \bar{G}id + \bar{G}r \tag{2.6}$$

Where:

$\bar{G}d$: Direct irradiance where the solar rays go straight from the sun to the array surface [kW/m2]

$\bar{G}id$: Indirect irradiance where the solar ray direction is changed by the atmosphere [kW/m2]

$\bar{G}$r: Reflected irradiance where the solar rays are reflected upon the PV array from the environments [kW/m2]

**Clearness index**

The clearness index is a measure of the clearness in the atmosphere and shows the fraction of radiation that hits the earth of the total radiation at the top of the atmosphere. It is used in order to find what percentage of the radiation that is diffuse and what is direct. This affects total irradiation on a tilted plane as the diffuse irradiation can come from all angles, while the beam irradiation will come directly from the angle of the sun to the module. The monthly average clearness index values are calculated in HOMER combining the site-specific irradiation with the cloud cover for the system location without giving the user opportunity to manually insert them. The software calculation method was not able to produce sensible values for the clearness index for Ny Ålesund as time of sunset and sunrise are used in the calculation and are non-existent during the months experiencing polar day. In order to overcome this challenge, the city of Oslo (latitude: 59°54’45” N, longitude: 10°44’45”E) was set as location for cloud cover combined with the solar irradiation data for Ny Ålesund.

In table 1, a comparison between the clearness index values for Ny Ålesund calculated by using Oslo as cloud cover location in HOMER and SRB-values found on the POWER homepage for Ny Ålesund is displayed. The table shows clear similarities in the clearness index values, and especially in the months with the highest irradiation. The clearness index calculated by using Oslo as cloud cover location is therefore assumed valid.

*Table 1: Comparison between Clearness index values*

| Calculation method | Jan | Feb | Mar | Apr | May | Jun | Jul | Aug | Sept | Oct | Nov | Dec |
|---|---|---|---|---|---|---|---|---|---|---|---|---|
| Clearness index based on Oslo as location for cloud cover | n/a | 0,00 | 0,14 | 0,33 | 0,45 | 0,49 | 0,43 | 0,35 | 0,20 | 0,03 | n/a | n/a |
| Clearness index from SRB data for Ny Ålesund | n/a | 0,16 | 0,38 | 0,43 | 0,44 | 0,45 | 0,40 | 0,40 | 0,37 | 0,27 | n/a | n/a |

In figure 2.10 the monthly average solar global horizontal irradiation for Ny Ålesund and the clearness index is shown graphically. The data used for solar irradiation is taken from the NASA SRB. The figure shows a minimum and maximum monthly average solar global horizontal irradiation of 0,01 kWh/m2/day (Feb) and 5,56 kWh/m2/day (Jun) respectively. The months November through January experiences no sun due to polar night. The scaled annual average global horizontal irradiation is at 1,84 kWh/m2/day.

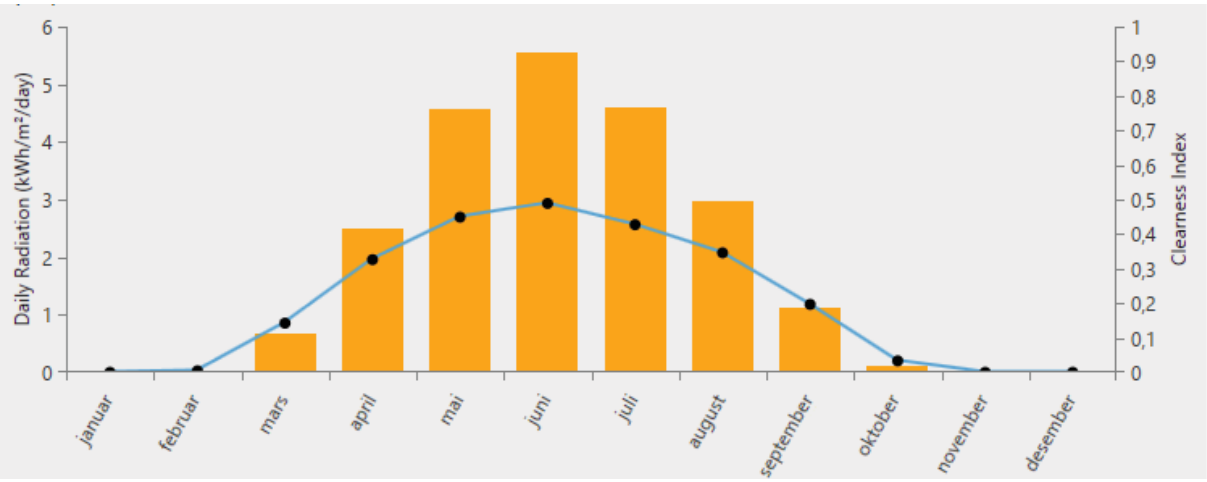


*Figure 2.10: Annual average monthly daily radiation and clearness index as represented in HOMER*

**Solar irradiation data uncertainty**

The surface meteorology and solar energy methodology manual (NASA, 2006) describes the difference between the mean of the respective solar radiation values for SRB and the BSRN. Daily total surface irradiance at the BSRN sites in regions above 60 degrees latitude, north and south (i.e. 60 degrees poleward) has a bias of -0,2039. This means that the satellite data on average overestimates the daily irradiance by 0,2039 kW/m2 compared to the measurements from the more accurate BSRN. The satellite data values gathered for Ny Ålesund are similar to values reported by Kejna et al. (2017). In their article, an annual average daily irradiation of 1,78 kWh/m2/day is presented based on BSRN measurements between july 2013 and August 2013. The time-scope for these values is only one year, and as they are comparable to the satellite data with time-scope of 22 years, the dataset with the greater time-scope was used in the simulation. As there are some uncertainties concerning the exact values of clearness index and solar irradiation for Ny Ålesund, solar irradiation was added as a sensitivity factor considering a 25% negative or positive deviation.

**Reflected irradiation**

When the solar module is tilted, solar irradiation will be reflected upon the PV array from the ground and surroundings due to the albedo affect. This type of irradiation is called reflected irradiation and must be added to the diffuse and direct radiation to give a complete measure of total solar insolation incident. Figure 2.11 represents measured Albedo in Ny Ålesund in the time period 1981 to 1997 and table 2 shows the average albedo fraction for each month of the year as described by Winther et al. (2002). November to February is excluded from the table as no or close to no irradiation is received in these months.

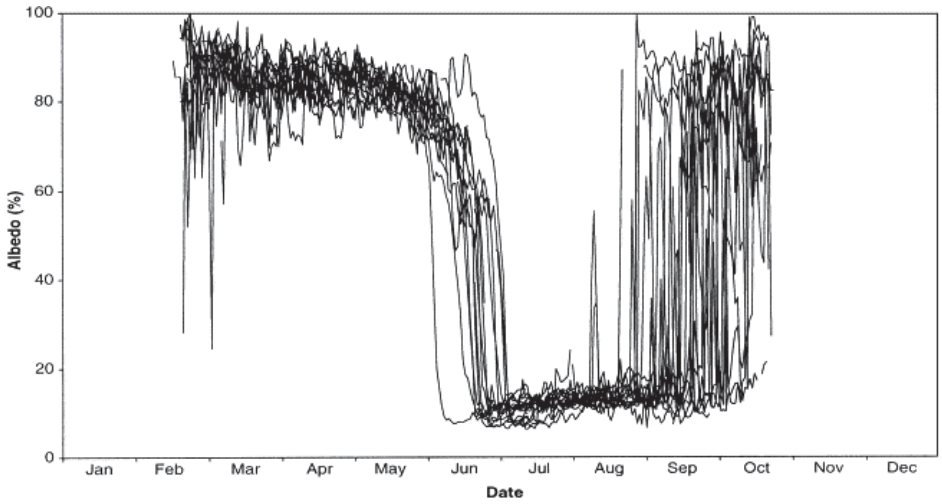


*Figure 2.11: Measured Albedo in Ny Ålesund between 1981 and 1997*

*Table 2: Description of Albedo levels in Ny Ålesund*

| | Kwh/m2/day | Percentage of total annual irradiation received | Albedo | |
|---|---|---|---|---|
| March | 0,67 | 3 % | 80 % | 0,024264 |
| April | 2,5 | 11 % | 80 % | 0,090539 |
| May | 4,57 | 21 % | 75 % | 0,155161 |
| June | 5,56 | 25 % | 45 % | 0,113264 |
| July | 4,6 | 21 % | 15 % | 0,031236 |
| August | 2,97 | 13 % | 15 % | 0,020167 |
| September | 1,12 | 5 % | 40 % | 0,020281 |
| October | 0,1 | 0 % | 40 % | 0,001811 |
| | | 100 % | Average albedo | 46 % |

From table 2, an annual average albedo of 46% is calculated by weighting the monthly albedo with the percentage of sun received in the respective month. The annual average albedo derived from this method is similar to an albedo value of 47% reported by Xianwei and S. (2011) for the time period 2003 to 2008. HOMER uses 20% as standard value for ground reflection (albedo). The reason why measurements from Ny Ålesund show much higher values is due to snow covering the ground in large parts of the year with the most likely dates for beginning of snowmelt and snow arrival being June 5th and September 17th respectively. The average albedo for Ny Ålesund is therefore set at 46% in the simulation software instead of the default value of 20%.

**Azimuth and tilt angle**

The orientation and tilt of the PV array affects performance output as it decides how much of the direct, diffuse and reflected irradiance will enter the panel. Orientation is described by the panel's azimuth angle which is usually set to 0 degrees (directly south) in the northern atmosphere in order to maximize output (Messenger & Ventre, 2005). The tilt angle describes the angle between the surface of the panel and a horizontal plane, and the general rule for optimal tilt angle to optimize for energy production is at 90% of the site latitude. In addition, one can optimize tilt angle for winter and summer by decreasing or increasing the tilt angle by 15 degrees respectively (Messenger & Ventre, 2005). As there is no light in winter, it only makes sense to tilt the panels for summer optimization. The tilt angle was therefore set at 56,1 degrees.

## 2.5 Elements in the Hybrid Energy System

The different system components shown in figure 2.12 will be described in the chapter 2.5.1.

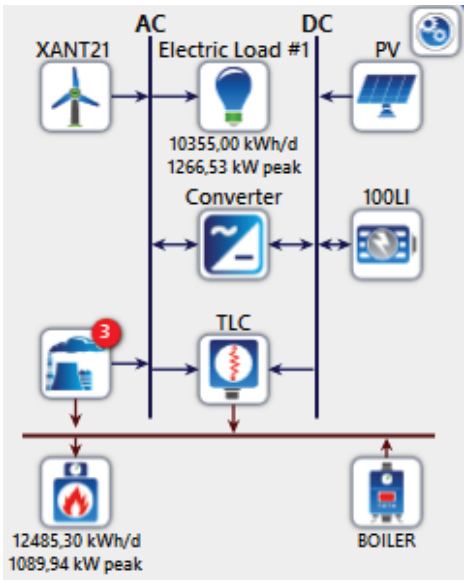


*Figure 2.12: A system overview of the different system components used in the simulation*

### 2.5.1 Choice and cost of components

**PV module**

The "Generic flat plate PV" module without tracking system available in the HOMER element library was used in the simulation. Each unit has a rated power of 1 kW, a temperature coefficient of -0,5 %/°C, and 17,5 % efficiency. A standard derating factor of 80% is assumed, meaning that the panel will be able to give 80% of the output compared to output at test conditions due to shading, wiring losses and more. The derating factor parameter in the simulation tool only considers the temperature independent part of the derating factor as the temperature dependent part is modelled endogenously based on the temperature in each time-step.

**Converter**

Converters serve to convert the current from DC to AC when power is flowing into the local electric grid from batteries and solar modules and from AC to DC when power is to be stored in the batteries from the grid. A standard "System converter" with 95% efficiency from the HOMER catalogue was chosen for the simulation. In order to find the optimal converter size, one unit was given a capacity of 1 kW.

### Battery

The battery element will serve as short term power storage in times when the renewable power sources produce excess electricity, meaning more than what is demanded by the load and more than what the thermal load controller is able to convert to the heat load. A "Generic 100kWh Lithium ion battery package" from the HOMER catalogue was selected for the model simulation. This battery has a nominal voltage of 600 V, nominal capacity of 167 Ah, roundtrip efficiency of 90% and a maximum charge and discharge current at 167 A and 500 A respectively.

### Wind turbines

The wind turbine used in the model simulation is called XANT 100kW M-21 and is produced by an emerging Belgian turbine company named XANT. The company specializes in small and efficient turbines for use in remote and environmentally demanding areas and have been tested in micro-grids along the Scottish coast and a few other locations (XANT, 2017). There are several benefits of using this wind turbine for the energy system in Ny Ålesund. It is friendly towards natural landscape and possibly local bird- and wildlife with its low hub height, it has a small rotor diameter and low noise, and it can handle extreme weather conditions which the area might be prone to. Furthermore, the whole turbine with stem and rotors is transported in containers and can be constructed without the use of cranes or other demanding infrastructure, and maintenance is not supposed to last more than one day a year according to the manufacturer. Technical specifications are shown in table 3.

*Table 3: Technical specifications are gathered from the manufacturer's "General specification sheet" (XANT, 2018)*

| Technical Specifications XANT 100kW M-21 | |
|---|---|
| Rated electrical power | 100 kW |
| Cut-in Wind speed | 3,0 m/s |
| Rated Wind speed | 11 m/s |
| Cut-out Wind speed | 20 m/s |
| Rotor diameter | 21 meters |
| Number of blades | 3 |
| Hub Height | 31,6 meters |
| Total height | 42 meters |

### Diesel generator

Three diesel power generators were included in the model simulations. These are Mitsubishi S6R2-T2MPTK 423kW generators that produce electrical energy with approximately 27% heat recycling. The heat recycling ratio was derived from available statistics from the Kings Bay power station data sets. In order to get the closest approximation in generator specifications to the on-site generator already in place, a custom generator based on the Mitsubishi S6R2-T2MPTK Technical specifications brochure was added to the simulation software. Where no information was available, the default settings from a "Generic 500kW fixed capacity generator" available in the HOMER catalogue was used. Table 4 describes technical specifications of the generator in the simulation.

*Table 4: Technical specifications for the generator system element*

| Technical Specifications Diesel Generator | |
|---|---|
| Name | Mitsubishi S6R2 T2MPTK |
| Capacity | 423 kW |
| Fuel curve slope | 0,239 L/hr/kW |
| CO2 – Emissions* | 0,72 kg/L fuel |
| Minimum load ratio | 25% |
| Heat recovery ratio | 26,29% |

*Homer Calculates CO2 emission as all carbon content not emitted as unburnt carbon or carbon monoxide.

All three generators are already in place in the existing energy system and thus their capital cost was set to 0 NOK. The generators run on diesel, and as Svalbard are exempt from taxes, the diesel price is low despite high delivery costs. A diesel price of 9 kr/litre was given by the power station manager. As reported by IEA (2017) in the market report "Oil 2017", crude oil price is subject to several variables and hard to predict. As diesel price is an important variable cost in the system, fuel price was added as a sensitivity variable in the simulation.

### Boiler

The oil boiler is used to serve the heat load when there is no excess electricity or not enough heat recycling from the diesel generators to serve the demand. The Boiler element in HOMER is part of the "Combined heat and power module", and only a generic boiler is available in the catalogue. Emission variables were set equal as for the diesel generator and it was given a power efficiency of 85%. By optimization, the boiler will take the size needed to fulfil the remaining heat demand when other power sources are unavailable.

**Thermal load controller (TLC)**

The Thermal load controller (TLC) is also part of the “Combined heat and power module” and functions as an electric boiler in the system design. The thermal load controller uses excess electricity in the system to feed the heat load demand. The thermal load controller might serve an important role in increasing the renewable fraction in the hybrid energy system as the renewable technologies only produce electrical energy. By allowing renewable power sources to serve the heat load, the TLC will help decrease local pollution by replacing energy produced by diesel combustion. As a 225kW electric boiler manufactured by “Varmeteknikk AS” is already in place at the power station, the same specifications were used for the TLC as for the existing boiler. The initial installment cost was set to zero.

## 2.6 Economics

### 2.6.1 Investment costs, variable costs, and lifetime

The different system element costs are presented in table 5. The prices for the generic elements PV, converter, and battery are average prices given by various third-party sources. Third party sources were also used in order to find average prices for the wind turbine and diesel engine as the manufacturers’ prices were unavailable. International or American (US) price averages were considered due to their recent publication and when lacking Norwegian sources. The installment cost for the TLC was assumed equal to the existing electric boiler and acquired through a phone call with the manufacturer. The simulation software did not allow a price input for the diesel boiler. Svalbard is subject to substantial tax exemptions due to its remoteness from the Norwegian mainland. These exemptions are not considered in the system element costs.

*Table 5: System element costs are displayed. All prices found in dollars or pound were converted at exchange rate: 7,82 NOK/$ and 11,03 NOK/GBP (gathered from DNB 23.04.2018). Recovery cost is considered the same as the capital cost for all system elements.*

| System element | Capital and Recovery cost | Operation and Maintenance cost | Lifetime | Sources |
|---|---|---|---|---|
| 1 kW generic flat plate PV | 12 823 NOK | 117 NOK/year | 25 years | "U.S. Solar Photovoltaic System cost benchmark" (Fu et al., 2017) |
| 1 kW system converter | 782 NOK | - | 15 years | U.S. Solar Photovoltaic System Cost Benchmark (Fu et al., 2017) |
| 100 kWh lithium ion battery | 177 500 NOK | 1 775 NOK/100kwh/year | 15 years | "Electrifying insight: How automakers can drive electrified sales and profitability." (McKinsey&Company, 2017) |
| 100 kW XANT-21 wind turbine | 1 524 747 NOK | 39 878 NOK/year | 20 years | "Renewable power generation costs 2017" (IRENA, 2018) |
| Generator 423KW | 3 377 325 NOK | 78,2 NOK/hour<br>Diesel price: 9 NOK/litre<br>Usage: 0,239 litre/hour/kW | 30 000 hours of use | (EIA, 2017)<br>(HOMERsupport, 2018)<br>Personal communication with "Kings Bay AS". |
| TLC 225kW | 100 000 NOK | - | - | Personal communication with «Vameteknikk AS» |

### 2.6.2 Interest rate, inflation, and project lifetime

The Norwegian ministry of finance states that "the discount rate is the social economic alternative cost of binding capital in an investment and it should reflect the investment return from the best alternative of investment" (Finansdepartementet, 2014). It is an important element in economic calculations, and it is furthermore suggested to use a real discount rate of 4% for governmental investments with less than 40 years of lifetime (NVE, 2015). As Kings Bay AS is operating on behalf of the Norwegian government, the investment can be considered governmental, and a 4% real interest rate is therefore used in the model simulation.

Equation 2.7 is used to decide real interest rate with inflation and nominal discount rate as input variables.

$$i = \frac{i' - f}{1 + f} \tag{2.7}$$

Where:

$i$: Real discount rate [4%]

$i'$: Nominal discount rate [%]

$f$: Expected inflation rate [2,1%]

Based on historical data between 2006 and 2018 from the Norwegian national bank, the inflation rate is set to 2,1% (NOR, 2018). Using these rates, the nominal discount rate is calculated as 6,2%.

Lifetime of the project was set to 20 years in the simulation as this equals the assumed lifetime of the wind turbine. The wind turbine is the system element with the highest capital cost per kW installed, and the project lifetime was set so that a new system design can be considered at the end of its lifetime.

### 2.6.3 Net present cost (NPC) and Levelized Cost of Energy (LCOE)

The simulation software uses Net present cost (NPC) as a metric to compare and rank different energy systems during the simulation. The net present cost is the present value of all installment and operational costs minus the total present value of all revenues earned during the system lifetime (HOMER manual). Net present cost is calculated both for each system component individually and the system as a whole. The discounted salvage value of each component will be subtracted from the total costs. The different feasible system solutions will be ranked so that the system with the lowest NPC is presented as the most optimal solution.

Another useful metric is the levelized cost of energy (LCOE), used to compare different methods of energy generation. The LCOE is the assessment of the total lifetime cost of the electricity generation divided by total lifetime energy output. In order to calculate the LCOE, the capital recovery factor (CRF) and annual total cost must be found. The CRF is a ratio used to calculate the present value of an annuity and found through equation 2.8.

$$CRF(i,N) = \frac{i(1+i)^N}{(1+i)^N - 1} \quad (2.8)$$

Where:

$i$: The real discount rate [4%]

$N$: Project lifetime [20 years]

The CRF is used to calculate the total annualized cost ($C_{ann,tot}$), which is the annualized value of the total net present cost (equation 2.9).

$$C_{ann,tot} = CRF(i,N) * C_{NPC,tot} \quad (2.9)$$

Where:

$C_{NPC,tot}$: The total net present cost [NOK]

After finding total annualized cost, HOMER calculates the LCOE using equation 2.10. Notice that HOMER only calculates levelized cost of electricity, not including heat energy.

$$LCOE = \frac{C_{ann,tot} - c_{boiler} H_{served}}{E_{served}} \quad (2.10)$$

Where:

$C_{boiler}$: Boiler marginal cost [kr/kWh]

$H_{served}$: Total thermal load served [kWh/year]

$E_{served}$: Total electrical load served [kWh/year]

### 2.6.4 Emission costs

Svalbard and Ny Ålesund are exempt from most taxes including emission tax. In order to penalize release of carbon dioxide emissions from diesel combustion, rates for CO2 emissions were given as if the simulated power system was part of the EU ETS quota scheme.

The penalty was set at 200 NOK per tonne of CO2 emission in accordance with Statnett's long term market analysis for the power sector (Bøhnsdalen et al., 2016). The CO2 emission from combustion in the diesel generator and boiler was set to 13,566 g/liter as suggested by the software.

# 3. Results

The optimal system results derived from the economic inputs, technology choice and resource availability presented in chapter 2 are displayed through a series of tables and figures in chapter 3.1. Furthermore, a comparison between the proposed optimal hybrid power system and the current diesel power system in place at Ny Ålesund is given. Chapter 3.2 explores how NPC and system renewable energy fraction respond to changes in the three sensitivity variables described in chapter 2.2.1. No feasible system solution was found when optimizing with consideration to the 20% minimum renewable energy constraint within the model configurations. This will be deliberated further in chapter 4.2.

## 3.1 Results from system optimization

Table 3.1 and 3.2 displays the power capacities, energy output, NPC, LCOE, fuel usage and renewable fraction for the optimal solution based on diesel price of 9 NOK/litre, average annual global solar irradiation at 1,84 kWh/m2/day, and average annual wind speed at 4,01 m/s.

*Table 3.1: A presentation of key result parameters in the optimal solution*

| System results | |
|---|---|
| **Net present cost (NOK)** | 185 137 700 |
| **Levelized cost of energy (NOK/kWh)** | 2,24 |
| **Installed capacity generator (kW)** | 1269 |
| **Installed capacity PV (kW)** | 470 |
| **Installed capacity wind turbine (kW)** | 300 |
| **Size battery (kWh)** | 300 |
| **Installed capacity TLC (kW)** | 225 |
| **Installed capacity converter (kW)** | 470 |
| **Annual fuel usage (litres)** | 1181481 |

*Table 3.2: A presentation of power outputs and energy contribution fractions by power source*

| Unit output | Diesel boiler (kWh) | Generator heat retrieval (kWh) | Generator electricity (kWh) | PV (kWh) | Wind turbine (kWh) | TLC (kWh) |
|---|---|---|---|---|---|---|
| **Energy served** | 3 312 960 | 1 238 757 | 3 104 223 | 273 421 | 463 086 | 5479 |
| **Percentage of electrical energy served** | - | - | 80,8 % | 7,1 % | 12,1 % | - |
| **Percentage of heat energy served** | 72,7 % | 27,2 % | - | - | - | 0,1 % |
| | **Fossil** | | | **Renewable** | | |
| **Percentage of total energy served** | **91,16 %** | | | **8,84 %** | | |

As presented in table 3.2, the renewable fraction of the total heat and electrical energy served is at 8,84%. The renewable fraction of total electrical energy served and total heat energy served is at 19,2% and 0,1% respectively. The renewable energy served to the thermal load is produced through the thermal load controller feeding on excess electrical energy from the electric grid.

Figure 3.1 and 3.2 show monthly average loads for heat and electrical energy production by the selected optimal hybrid energy system. Notice how the energy generated by the TLC is excluded due to its insignificant contribution.

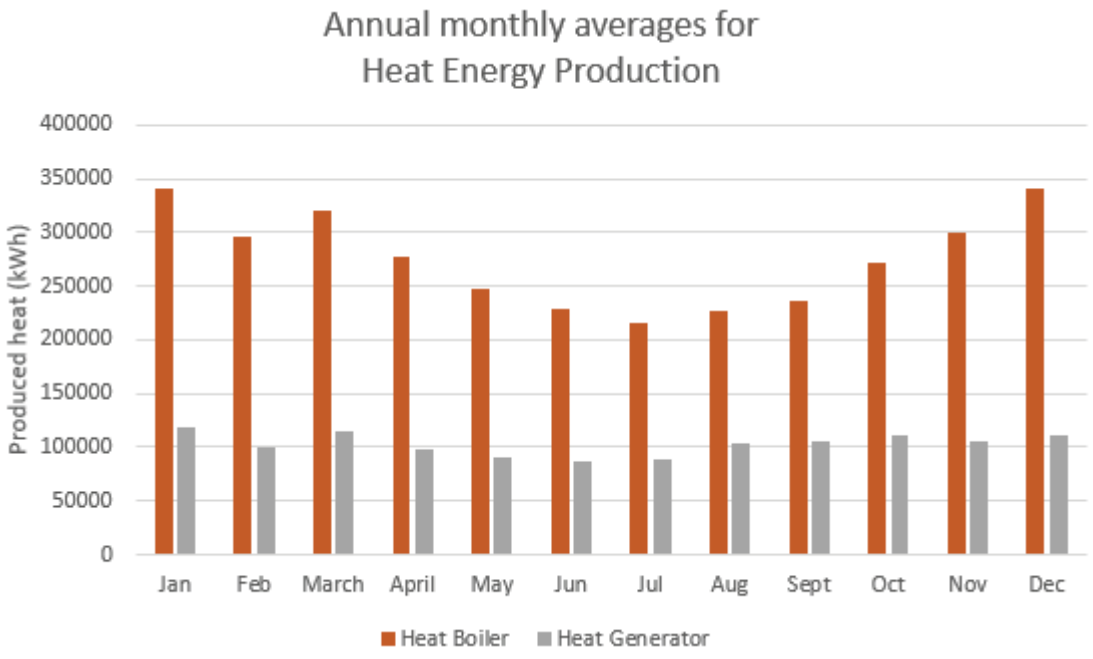


*Figure 3.1: Annual monthly averages for heat energy served for the generator and diesel boiler*

The month with the highest heat energy production is January for the diesel generator and December for the diesel boiler. While the diesel generator contributes with fairly similar energy yield throughout the year, the diesel boiler production pattern follows a patter negatively correlating to the site temperature displayed in figure 2.9.

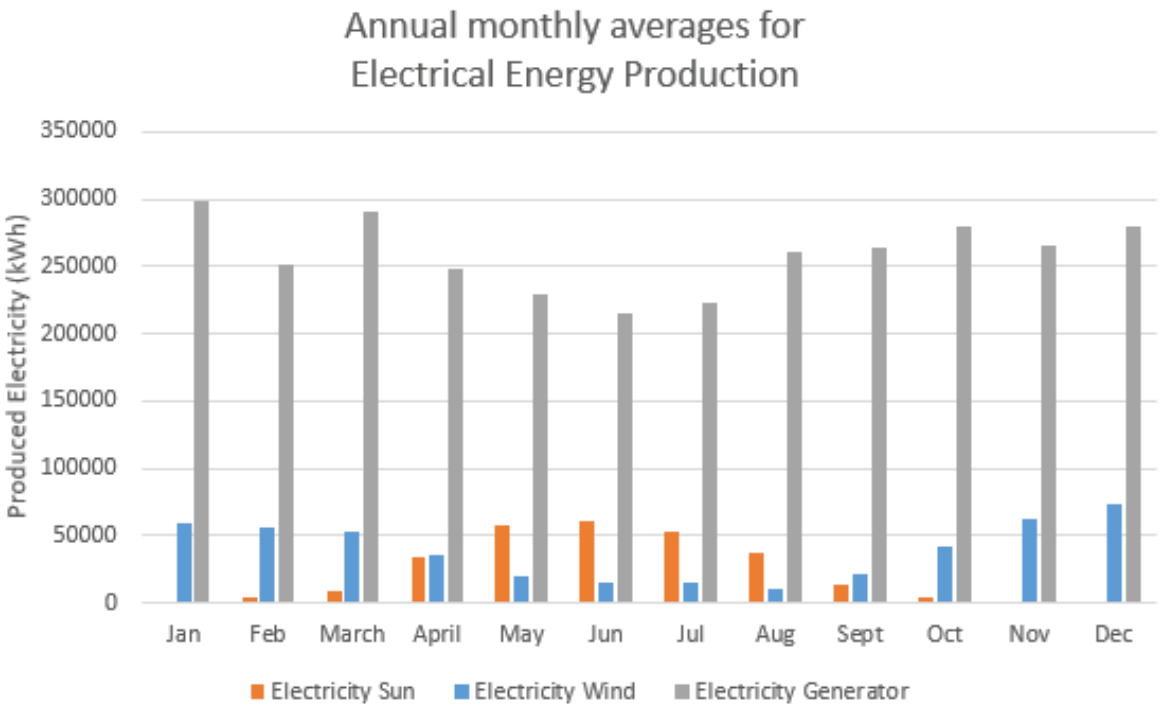


*Figure 3.2: Annual monthly averages for electrical energy served for PV, wind turbine and diesel generator*

As seen in figure 3.2, wind and solar energy production compliments each other as solar yield is higher in summer while the wind yield is higher in winter. This reduces the degree of system over-sizing.

Figure 3.3 shows annual monthly averages for fuel usage and renewable fraction. The two metrics shows a negative correlation as increased use of renewable energy replaces diesel consumption. The proposed power system experiences the highest renewable fraction values in the summer season with a peak of 12,6% in June, and lower values in fall and spring with the lowest being at 5,5% in September.

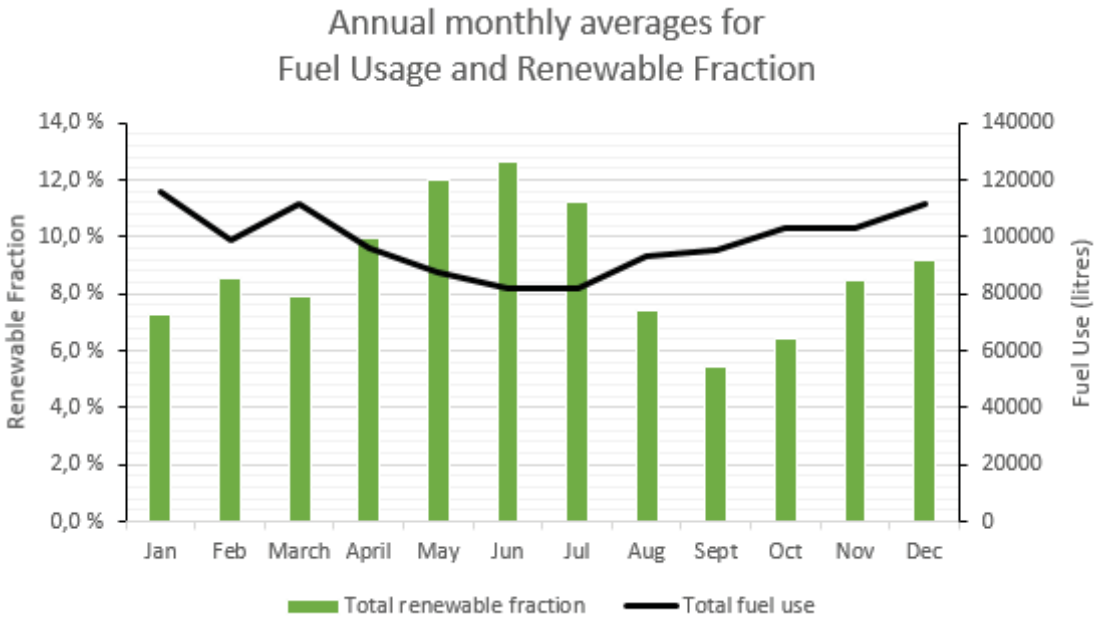


*Figure 3.3: Annual monthly averages for fuel usage and renewable fraction*

Table 3.3 shows a comparison of the hybrid energy system with the base system. As previously stated, the base system is the power system currently in place and solely consists of the three generators, the thermal boiler and the thermal load controller.

*Table 3.3: A comparison of the new suggested system and the base system currently in place*

| **Comparison to base system** | | | |
|---|---|---|---|
| | **Base system** | **New system** | **Difference** |
| NPC (kr) | 200 680 506 | 185 137 700 | -15 542 806 |
| LCOE (kr/kwh electric) | 2,54 | 2,24 | -0,3 |
| Initial capital costs (kr) | 0 | 11 500 000 | 11 500 000 |
| Nominal operating costs (kr/yr) | 14 800 000 | 12 800 000 | -2 000 000 |
| Fuel Use (L/Y) | 1328715 | 1181481 | -147234 |
| Emissions (kg/year) | 958801 | 852557 | -106244 |

The negative values in the “Difference”-column describes savings by implementing the hybrid energy system presented as the optimal power solution in this thesis. The initial capital cost for the base system is set at zero as the system already is in place.

Figure 3.4 shows the discounted cumulative cash flows over the project lifetime for the current system and the base case and was retrieved from the optimal solution report in the simulation software.

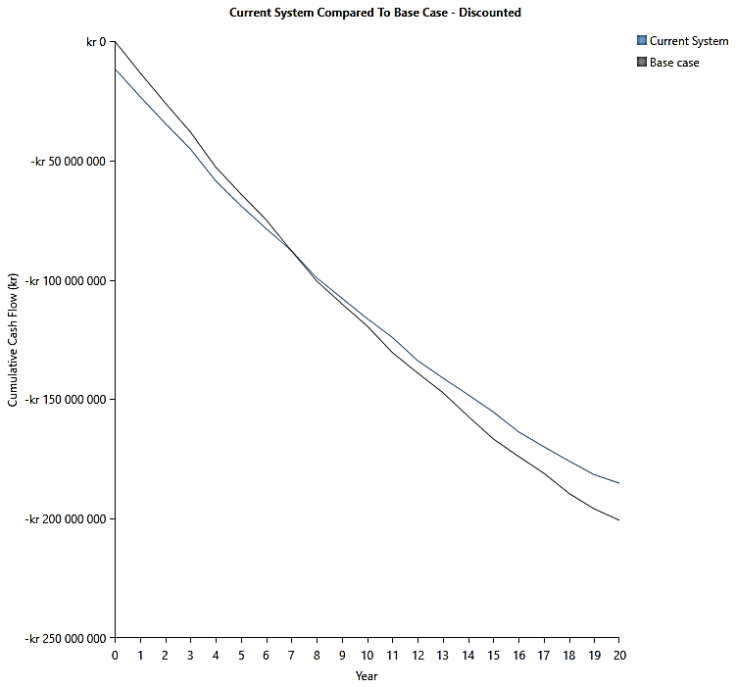


*Figure 3.4: Discounted cumulative cash flows over project lifetime for the suggested system and the base scenario*

The discounted payback of investing in the suggested system instead of keep using the base scenario is at 7 years as can be seen in figure 3.4. The HOMER result report states an internal rate of return for the project investment at 15,1%. Considering that the Norwegian ministry of finance suggests a rate of return of 8% for high-risk investments (Finansdepartementet, 1999), the suggested project lies well within what can be recognized as sound investment.

## 3.2 Sensitivity analysis

Three sensitivity variables were chosen in order to investigate the impact on deviations from their assumed values on different metrics and parameters in the optimal system solution. As seen in figure 3.7, the NPC is most sensitive to changes in diesel price where a 50% positive or negative change, would change net present cost with around 60 million NOK respectively. Figure 3.8 displays that the renewable energy fraction is more sensitive to wind strength in terms of increase, as a 25% increase in wind speed would result in more than doubling the renewable fraction. In terms of reduction of renewable fraction, annual average irradiation has more impact as a 25% decrease in solar irradiance would reduce the renewable fraction by 35%.

The sensitivity of LCOE is not displayed as it is dependent on NPC, just as the sensitivity of fuel use and CO2-emission are not displayed as they are dependent on the renewable fraction in the system.

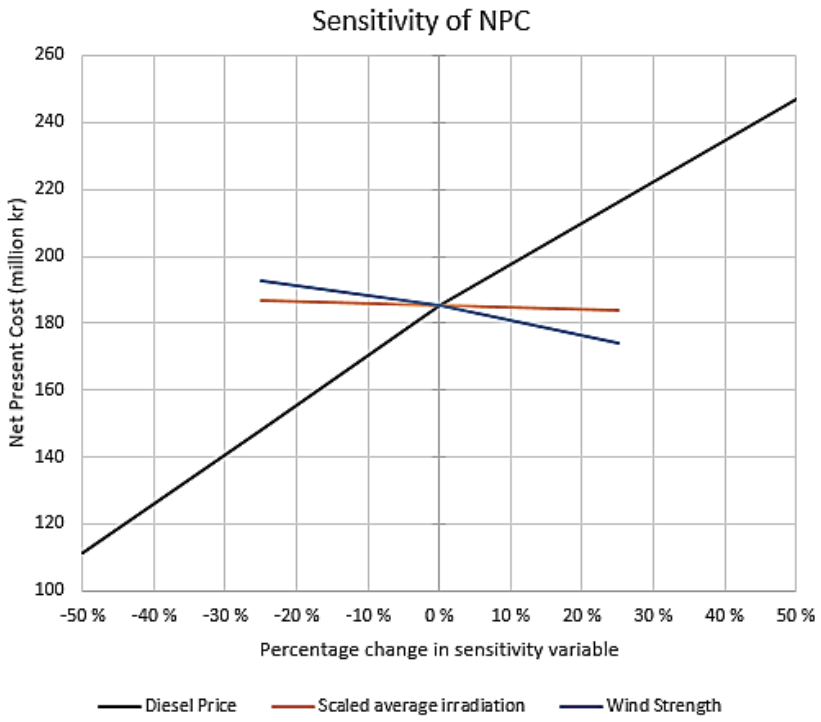


*Figure 1.7: Sensitivity chart for net present cost of the optimal solution*

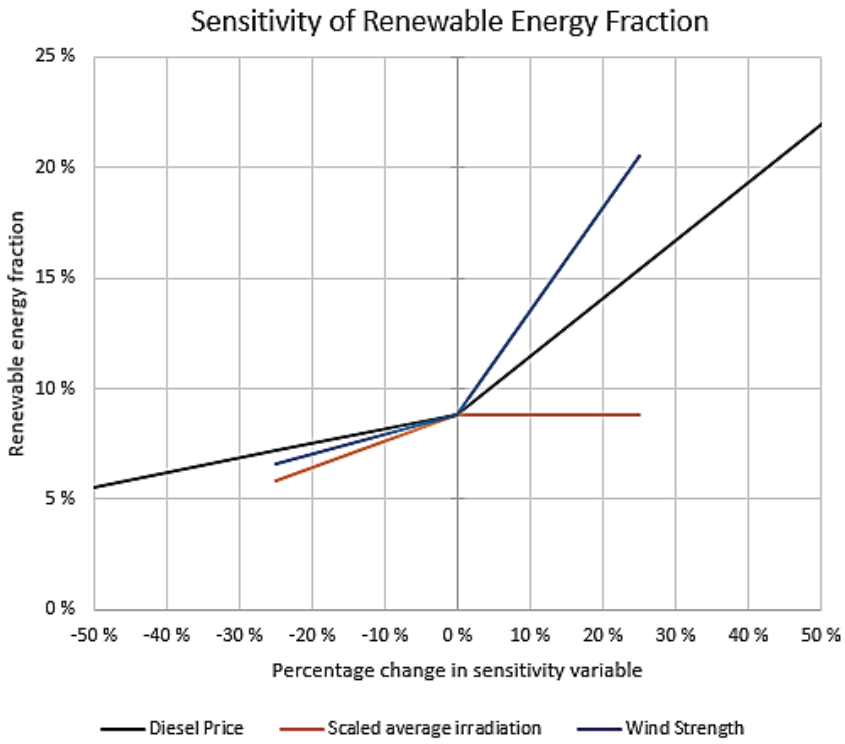


*Figure 3.8: Sensitivity chart for the renewable fraction of the optimal solution*

# 4. Discussion

## 4.1 General comments

The system simulation conducted in this thesis only offers an approximation of the real energy system. There are several assumptions included in the model such as the specifications of the general system elements provided in the software catalogue for solar module, inverter and battery. Furthermore, the generators used in the simulation are generic 423 kW diesel generators and do not necessarily share all the same specifications as the "Mitsubishi S6R2-T2MPTK 423kW" that are used in the current energy system. Even though it was possible to insert parameter inputs and increase the similarity between the generators, the possible specification deviations might cause different optimization results.

Capital costs, operation and management cost, replacement cost and salvage revenue for the system elements were in most cases inserted based on average prices from third party agencies. More accurate pricing could have been accessed directly through contractors, and consideration to the tax exempts on Svalbard were not considered. As the renewable technologies are considered to have high investment costs and low variable costs, consideration to tax exempts would favour the renewable technologies. It is also important to note that this thesis has considered zero capital costs for the existing generators as they are in place and functioning, but they were still considered to function for the full life-time as if they were new.

Sensitivity values were limited by the computer hardware used to run the simulations. When including the nine sensitivity values that were used in the simulation (three values for each variable), the optimization process lasted for close to twelve hours. As several simulation re-runs with minor input or element adjustments in the system model were needed after reviewing and gaining more knowledge about the simulation resources and element specifications, time became a limiting factor when choosing which sensitivity variables to consider. The probability of change in the different sensitivity variables was not considered.

## 4.2 Software limitations

Of the 970 877 simulations for system solution considered in the optimization process by the simulation software, 660 785 of them were infeasible due to the thermal load controller. It was assumed that the TLC would function as a form for electric boiler that could transfer electrical energy to heat energy. Inclusion of such an element would assumedly favour more renewable energy production in the system, but when activated, the optimization ends up suggesting lower

values of renewable energy. In addition, with the TLC activated, it optimizes the system so that very little excess energy (only 5479 kWh annually) is available for conversion to serve the thermal load. This even though the marginal cost for renewable energy is much lower than energy from diesel. Considering the low instalment cost for the TLC, the huge constraint it sets on feasible system solutions seems unreasonable.

By running HOMER with the thermal load controller element included and thus allowing conversion from electric to heat energy, but without consideration to price or capacity, the results varied greatly from those presented in chapter 3. Table 4.1 displays the optimization results for the model including minimum renewable energy constraints of 20%, 50%, 80% and 100%. By not including the TLC price and capacity, the optimal system with zero constraints on renewable fraction was equal to the system with the 20% minimum renewable constraint. No feasible system solutions were found when minimum renewable fraction constraint was set to 100%.

*Table 4.1: A display of key result parameters for the optimal solutions with different constraints considering minimum renewable fraction*

| System results | | | |
|---|---|---|---|
| **Minimum renewable fraction constraint** | **20 %** | **50 %** | **80 %** |
| **NPC (NOK)** | 163 594 400 | 169 024 700 | 185 137 700 |
| **LCOE (NOK/kWh)** | 1,82 | 1,92 | 7,10 |
| **Capacity diesel generator (kW)** | 1 269 | 1 269 | 1 269 |
| **Capacity solar PV (kW)** | 1 146 | 1 748 | 7 678 |
| **Capacity wind turbine (kW)** | 2 200 | 3 000 | 14 200 |
| **Size battery (kWh)** | 2 800 | 4 600 | 6400 |
| **TLC mean output (kW)** | 166 | 304 | 4017 |
| **Capacity converter (kW)** | 696 | 837 | 1 930 |
| **Annual fuel usage (litres)** | 691 116 | 549 091 | 201 695 |
| **Renewable energy fraction** | 49 % | 61 % | 95 % |
| **Excess energy (kWh)** | 559 230 | 1 276 815 | 19 557 695 |

The simulation software does not consider excess electricity as part of the renewable fraction when optimizing within the constraints.

As the TLC will convert excess electricity into thermal energy, excess electrical energy minus excess thermal energy is included as part of the total renewable energy served. This is assuming that all excess electricity as well as excess heat comes from renewable sources. Looking at table 4.1, excess energy increases substantially with higher constraints on the minimum renewable energy fraction. This implies system oversizing, as much of the energy produced must be dumped instead of used to provide energy services. The reason for the rising excess electricity is mainly due to the substantial variations in monthly maximum and minimum values used by the simulation software and the seasonal variations in renewable power resource for wind and solar. I order to fulfil high minimum renewable constraints, the capacity of renewable power technology must be substantial for the periods experiencing low resource availability. The excess electricity could possibly to a higher degree be stored in batteries or other storage elements, but this would according to the software be at the expense of the total NPC of the project. Incorporating production and use of hydrogen in the system simulation could be considered in further studies in order to achieve improved annual energy balance.

## 4.3 Natural limitations

No study of the physical limitations considering placement of system elements or the impact for existing natural and cultural landscape were done in the study. Simulating without constraint on upper limits on number of windmills, batteries and solar modules could give results that are not viable due to space limitations. The system with no consideration to TLC price and capacity and 80% minimum renewable fraction constraint showed in table 4.1 is an example of such a case as 142 turbines would not be physically feasible. Nor were consideration to cultural elements such as heritage sites or natural elements such as bird life and similar were not undertaken. The study only shows the economically optimal system, and only its direct costs were considered. Positive externalities such as the possibility of attracting more researchers, international attention and tourism was not considered.

## 4.4 Investment support

Countries all over the globe, including Norway, have developed programs for subsidization of renewable power production in order to push technology faster into the market and start climate mitigation. According to the international energy association, 82 billion dollars were given as subsidy for renewable electricity production in 2012, and annual subsidies are predicted to increase until a peak in 2035 (IEA, 2014). The proposed integration of renewable power solutions in Ny Ålesund is likely to receive subsidies, but these are not considered in the model simulation due to limitations of HOMER and lack of insight in the realistic subsidy amount. Due to collective political agreement and

several private business initiatives to support green solutions for Svalbard, there are many possibilities of achieving grants and subsidies for renewable energy projects. Table 4.2 displays a short list of possible providers of subsidies that could reduce project costs. Such subsidies would increase the viability of implementing renewable energy technology and should be considered compliments to the result presented in this thesis.

*Table 4.2: List of potential providers of subsidies for the suggested hybrid renewable-diesel energy system*

| Provider | Description |
|---|---|
| Svalbard's Environmental Fund | Since 01.04.2007, an environmental visitor tax of 150 NOK was implemented for Svalbard. The revenues are put in the the Svalbard environmental fund and are granted for projects promoting protection of the island's environment (Sysselmannen, 2012). |
| ENOVA | Enova is a governmental institution with responsibility of investing financial and advisory resources in order to promote a healthy climate, renewable energy and reduction of climate gases. ENOVA invests more than 2 billion NOK annually in green solutions all over Norway (ENOVA, 2018). |
| Norway 203040 | Norway 203040 is a business-driven climate cluster that works together with public authorities in order to reach the ambitious climate goals towards 2030. Finding innovative solutions towards a fossil free Svalbard is one of the main focus areas (Norge203040, 2018). |

# 5 Conclusion and recommendations

## 5.1 Conclusions

This thesis has explored the economic viability of introducing renewable energy power sources to the existing diesel power system in the isolated arctic town of Ny Ålesund in Svalbard. Based on the findings, some conclusive remarks are presented.

According to resource and element specification assumptions used in this research, implementation of solar PV and wind turbines as power sources in Ny Ålesund is economically beneficial with a total saving of 15,5 million NOK during the project lifetime of 20 years. The study thereby recommend that Kings Bay AS should invest in local power generation even if solely based on monetary values. The renewable energy fraction for the proposed energy system is calculated at 8,9%. Using energy from wind and solar power sources would therefore replace use of approximately 147,2 m3 of diesel and reduce emissions by around 106 tonnes of CO2 annually. Thus, the new energy system suggested in this thesis will leave the town with a greener energy footprint in addition to economic benefits.

From the optimization results, it is clear wind energy will contribute more to the renewable energy production than that of solar energy, with production of 463 086 kWh and 273 421 kWh respectively. The annual monthly output for these power sources peak at different times of the year and complements each other in a way that reduces the chance of exceeding power demand. Even with high seasonal variations in sunlight availability, solar energy is economically beneficial to include in the optimal energy system and contributes 7,1% of total annual electricity served in the town.

The most influential sensitivity variables were found for net present cost and system renewable energy fraction. The net present cost is most sensitive to changes in diesel price followed by wind speed and solar irradiation. The system renewable fraction is more sensitive to wind strength followed by diesel price in terms of an increase in renewable fraction and more sensitive to solar irradiance in terms of reduction in renewable energy fraction.

If no consideration is taken to the cost and capacity of the thermal load controller when optimizing for the best energy system, the simulation software presents an optimal solution with a levelized cost of energy at 1,82 NOK compared to 2,54 NOK in the base scenario. The renewable fraction for this system is at 49%, thereby reducing emissions and fuel use almost by half. Furthermore, the EU

goal that 20% of consumed energy should come from renewable energy is sustained. This energy system is vastly superior in monetary and environmental terms compared to the base system and the system taking the thermal load controller into consideration. Due to uncertainties in how the thermal load controller costs and capacity affects the software simulation, investments based on this simulation report should be taken with care.

Even so, there are reasons to believe that this thesis uses a cautious approach in terms of finding the most optimal energy system in terms of monetary and more indirect value. Some of the factors that might change the simulation outcome in favour of higher renewable fraction and lower system costs are (1) the potential subsidies and tax exemptions that could reduce cost of the renewable power production elements, (2) the unjustified limitations for system feasibility in the simulation process due to the thermal load controller constraints, (3) that the diesel generators are assumed full lifetime and no capital costs at project implementation, and (4) that the potential beneficial spill-over effects of reducing emissions were not considered .

## 5.2 Future research

In order to verify the findings of this thesis, other software analysis tools could be used with the same input assumptions. This is especially relevant due to how the thermal load controller element in HOMER affected the simulation feasibility to great extent without it being clear why.

Conduct a consequence analysis for implementation of wind turbines in Ny Ålesund. The installation and use of wind turbines might have negative consequences for birdlife, natural landscape or cultural heritage. A proper consequence analysis should consider these effects in comparison to the benefits of utilization in order to make sure that wind turbines are desired for energy harvest. In addition, proper investigation on what subsidies the project can gain from different contributors and negotiations with potential retailers should be performed in order to get more realistic cost assumptions.

Consider similar model simulations for the other settlements in Svalbard or other arctic areas. The results of this thesis support greater use of local renewable power sources in the arctic region and can potentially spark more interest for similar energy system solutions in other communities.

# List of References


Berdin, Khakimovich, V., Yulkin, Mikhailovich, G., Kokorin, A. O. & Yulkin, M. A. (2017). *Renewable energy in off-grid settlements in the Russian Arctic*: World Wildlife Foundation Russia.

BSRN. (2018). *Objectives of the Baseline Surface Radiation Network (BSRN)*: World Radiation Monitoring Center. Available at: http://bsrn.awi.de/project/objectives/ (accessed: 12.05).

Byun, Y.-H., Yoon, H.-K., Kim, Y. S., Hong, S. S. & Lee, J.-S. (2014). Active layer characterization by instrumented dynamic cone penetrometer in Ny-Alesund, Svalbard. *Cold Regions Science and Technology*, 104-105: 45-53. doi: https://doi.org/10.1016/j.coldregions.2014.04.003.

Bøhnsdalen, E. T., Västermark, L. K., Duskeland, I. H., Holmefjord, V., Aarstad, J. & Kringstad, A. (2016). *Langsiktig Markedsanalyse Norden*: Statnett.

Cisek, M., Makuch, P. & Petelski, T. (2017). Comparison of meteorological conditions in Svalbard fjords: Hornsund and Kongsfjorden. *Oceanologia*, 59 (4): 413-421. doi: https://doi.org/10.1016/j.oceano.2017.06.004.

Eeg-Henriksen, F. & Sjømæling, E. (2016). *This is Svalbard*: Statistics Norway.

EIA. (2017). *Construction cost data for electric generators installed in 2015*. Annual Electric Generator Report: U.S. Energy Information Administration.

ENERGY, H. (2018). *Learn more about HOMER Pro*. Available at: https://www.homerenergy.com/products/pro/index.html (accessed: 17.03).

ENOVA. (2018). *Om ENOVA*. Available at: https://www.enova.no/om-enova/ (accessed: 13.05).

Finansdepartementet. (1999). Behandling av diskonteringsrente, risiko, kalkulasjonspriser og skattekostnader i samfunnsøkonomiske analyser.

Finansdepartementet. (2014). Prinsipper og krav ved utarbeidelse av samfunnsøkonomiske analyser.

Fu, R., Feldman, D., Margolis, R., Woodhouse, M. & Ardani, K. (2017). *U.S. Solar Photovoltaic System Cost Benchmark: Q1 2017*: National Renewable Energy Laboratory.

Førland, E. J., Benestad, R., Hanssen-Bauer, I., Haugen, J. E. & Skaugen, T. E. (2011). Temperature and Precipitation Development at Svalbard 1900 to 2100. *Advances in Meteorology*, 2011: 14. doi: 10.1155/2011/893790.

Green, M. A., Hishikawa, Y., Warta, W., Dunlop, E. D., Levi, D. H., Hohl-Ebinger, J. & Ho-Baillie, A. W. H. (2017). Solar cell efficiency tables (version 50). *Progress in Photovoltaics: Research and Applications*, 25 (7): 668-676. doi: 10.1002/pip.2909.

HOMERenergymanual. (2014). *HOMER PRO 2.2.8 HELP MANUAL*: HOMER ENERGY.

HOMERsupport. (2018). *Diesel Operation & Maintenance costs*. Available at: http://usersupport.homerenergy.com/customer/en/portal/articles/2188634-diesel-o-m-costs (accessed: 16.04).

IEA. (2014). *World Energy Outlook 2013*. Paris: International Energy Agency.

IEA. (2016). *A Snapshot og Global PV*: The International Energy Agency (IEA).

IEA. (2017). *Oil 2017 - Forecasts to 2022*: International Energy Agency.

IRENA. (2018). *Renewable Power Generation Costs in 2017*. Abu Dhabi: International Renewable Energy Agency.

Islam, M. R., Mekhilef, S. & Saidur, R. (2013). Progress and recent trends of wind energy technology. *Renewable and Sustainable Energy Reviews*, 21: 456-468. doi: https://doi.org/10.1016/j.rser.2013.01.007.

Kaczmarska, M., Glowacki, P., Fleury, D., Flå, K., Gisnås, H. & Tangen, H. (2012). *Energy and data connection strategies for the four main land-based platforms*: Norwegian Polar Institute

Institute of Geophysics, Polish Academy of Sciences.

Kejna, M., Maturilli, M., Araźny, A. & Sobota, I. (2017). *Radiation balance diversity on NW Spitsbergen in 2010–2014*, vol. 38.

Mandelli, S., Barbieri, J., Mereu, R. & Colombo, E. (2016). Off-grid systems for rural electrification in developing countries: Definitions, classification and a comprehensive literature review. *Renewable & Sustainable Energy Reviews*, 58: 1621-1646. doi: 10.1016/j.rser.2015.12.338.

Manwell, J. F., McGowan, J. G. & Rogers, A. L. (2010). *Wind Energy explained: Theory, Design and Applicatin, 2nd Edition*: John Wiley & Sons.

Maturilli, M., Herber, A. & König-Langlo, G. (2015). Surface radiation climatology for Ny-Ålesund, Svalbard (78.9° N), basic observations for trend detection. *Theoretical and Applied Climatology*, 120 (1): 331-339. doi: 10.1007/s00704-014-1173-4.

Mayer, J. N., Philipps, S., Saad, N., Hussein, D., Schlegl, T. & Senkpiel, C. (2015). Current and future cost of photovoltaics. *Berlin: Agora Energiewende*.

McKinsey&Company. (2017). *Electrifying insights: How automakers can drive electrified vehicle sales and profitability*: McKinsey&Company Advanced Industries.

Messenger, R. A. & Ventre, J. (2005). *Photovoltaic Systems Engineering. 2nd edition.* Florida: CRC Press LLCXa.

Multiconsult. (2016). *Growth in the sun power market 2015*. Available at: https://www.multiconsult.no/vekst-i-solkraftmarkedet-i-2015/.

NASA. (2006). *NASA Surface meterology and Solar Energy: Methodology*: NASA.

NASA. (2018). *Front page*: NASA Atmospheric Science Data Center. Available at: https://eosweb.larc.nasa.gov/ (accessed: 06.04).

NOR. (2018). *Inflation indicators*: Norges Bank (accessed: 05.05).

Norge203040. (2018). *Våre fokusområder*. Available at: http://norge203040.no/themes/.

NVE. (2015). *Kostnader i Energisektoren*: Norges Vassdrags- og Energidirektorat

Obydenkova, S. V. & Pearce, J. M. (2016). Technical viability of mobile solar photovoltaic systems for indigenous nomadic communities in northern latitudes. *Renewable Energy*, 89: 253-267. doi: https://doi.org/10.1016/j.renene.2015.12.036.

Otovo. (2018). *Bli Nabostrømkunde*. Available at: https://www.otovo.no/grid/ (accessed: 06.04).

PANGEA. (2018). *BSRN Toolbox*: PANGEA. Available at: https://wiki.pangaea.de/wiki/BSRN_Toolbox.

POWER. (2018). Data Access Viewer. In *NASA*. Available at: https://power.larc.nasa.gov/data-access-viewer/.

Przybylak, R. & Arazny, A. (2006). Climatic conditions of the north-western part of Oscar II Land (Spitsbergen) in the period between 1975 and 2000. *Polish Polar Research*, 27 (2): 133-152.

Sibbitt, B., McClenahan, D., Djebbar, R. & Paget, K. (2015). Groundbreaking Solar Case Study. *High Performing Buildings*.

Sinha, S. & Chandel, S. S. (2014). Review of software tools for hybrid renewable energy systems. *Renewable and Sustainable Energy Reviews*, 32: 192-205. doi: https://doi.org/10.1016/j.rser.2014.01.035.

Sysselmannen. (2012). *Om Svalbard Miljøfond*. Available at: https://www.sysselmannen.no/Svalbards-miljovernfond/Toppmeny/Om-Svalbards-miljovernfond/ (accessed: 13.05).

Sysselmannen. (2016). *Implementation of Solar PV at Svalbard Airport*. Available at: https://www.sysselmannen.no/Svalbards-miljovernfond/Rapportar/Etablering-av-solcelleanlegg/ (accessed: 19.04).

Traa, K. (2017). *Svalbard can become the beginning of a new Norwegian energy adventure*: Energi og Klima. Available at: https://energiogklima.no/kommentar/svalbard-kan-bli-starten-pa-et-nytt-norsk-energieventyr/ (accessed: 02.05).

Winther, J.-G., Godtliebsen, F., Gerland, S. & Isachsen, P. E. (2002). Surface albedo in Ny-Ålesund, Svalbard: variability and trends during 1981–1997. *Global and Planetary Change*, 32 (2): 127-139. doi: https://doi.org/10.1016/S0921-8181(01)00103-5.

XANT. (2017). *The moon never sets on a XANT turbine*. Available at: http://xant.com/2017/12/ (accessed: 14.04).

XANT. (2018). *XANT M-21 General Specifications*. Brussels.

Xianwei, W. & S., Z. C. (2011). Arctic and Antarctic diurnal and seasonal variations of snow albedo from multiyear Baseline Surface Radiation Network measurements. *Journal of Geophysical Research: Earth Surface*, 116 (F3). doi: doi:10.1029/2010JF001864.

YR. (2018). *Ny Ålesund Weather station*: Norwegian Meteorologic Institute. Available at: https://www.yr.no/sted/Norge/Svalbard/Ny-%C3%85lesund_m%C3%A5lestasjon/ (accessed: 02.05).

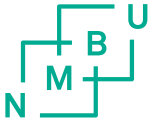


**Norges miljø- og biovitenskapelige universitet**
Noregs miljø- og biovitskapelege universitet
Norwegian University of Life Sciences

Postboks 5003
NO-1432 Ås
Norway